

คาร์บอนโมโนลิทที่เตรียมจากอาร์เอฟเจลและลิกโนเซลลูโลสที่ได้จากของเหลือทางการเกษตร

นายฤทธิไกร นามมูลสินธุ์

วิทยานิพนธ์นี้เป็นส่วนหนึ่งของการศึกษาตามหลักสูตรปริญญาวิทยาศาสตรมหาบัณฑิต

สาขาวิชาวิศวกรรมเคมี ภาควิชาวิศวกรรมเคมี

คณะวิศวกรรมศาสตร์ จุฬาลงกรณ์มหาวิทยาลัย

ปีการศึกษา 2554

ลิขสิทธิ์ของจุฬาลงกรณ์มหาวิทยาลัย

บทคัดย่อและแฟ้มข้อมูลฉบับเต็มของวิทยานิพนธ์ตั้งแต่ปีการศึกษา 2554 ที่ให้บริการในคลังปัญญาจุฬาฯ (CUIR)

เป็นแฟ้มข้อมูลของนิสิตเจ้าของวิทยานิพนธ์ที่ส่งผ่านทางบัณฑิตวิทยาลัย

The abstract and full text of theses from the academic year 2011 in Chulalongkorn University Intellectual Repository(CUIR)

are the thesis authors' files submitted through the Graduate School.

CARBON MONOLITH FROM RF GELS AND LIGNOCELLULOSIC  
MATERIALS FROM AGRICULTURAL WASTES

Mr. Rittikrai Nammoonsin

A Thesis Submitted in Partial Fulfillment of the Requirements  
for the Degree of Master of Engineering Program in Chemical Engineering

Department of Chemical Engineering

Faculty of Engineering

Chulalongkorn University

Academic Year 2011

Copyright of Chulalongkorn University



ฤทธิกร นามมูลสินธุ์: คาร์บอนโมโนลิทที่เตรียมจากอาร์เอฟเจลและลิกโนเซลลูโลสที่ได้จากของเหลือทางการเกษตร. (CARBON MONOLITH FROM RF GELS AND LIGNOCELLULOSIC MATERIALS FROM AGRICULTURAL WASTES) อ.ที่ปรึกษาวิทยานิพนธ์หลัก: ผศ.ดร.ณัฐพร โทพานนท์, อ.ที่ปรึกษาวิทยานิพนธ์ร่วม: อ.ดร.อดิศักดิ์ ไสยสุข, 72 หน้า.

งานวิจัยนี้เป็นการศึกษาการละลายและรีเจนเนอเรทวัสดุลิกโนเซลลูโลสจากวัสดุเหลือทิ้งทางการเกษตร ในขั้นแรกได้ทำการศึกษาหาสภาวะความเข้มข้นที่เหมาะสมของตัวทำละลายผสมระหว่างโซเดียมไฮดรอกไซด์และไฮโดรเจนเปอร์ออกไซด์ที่จะใช้สำหรับการละลายเศษวัสดุลิกโนเซลลูโลส (ฟางข้าว, มัน, ใบบวบ, กาบหมาก) ซึ่งพบว่าที่ความเข้มข้นของโซเดียมไฮดรอกไซด์ความเข้มข้นร้อยละ 8 โดยมวลและไฮโดรเจนเปอร์ออกไซด์ความเข้มข้นร้อยละ 10 โดยมวล สามารถทำการละลายเศษวัสดุลิกโนเซลลูโลสได้ดีที่สุด นอกจากนี้สารละลายลิกโนเซลลูโลสทั้งหมดได้ถูกนำมาทำกริเจนเนอเรทด้วยกรดซัลฟิวริกความเข้มข้น 2 โมลต่อลิตร ซึ่งพบว่าวัสดุลิกโนเซลลูโลสที่รีเจนเนอเรทได้จากเส้นใยกาบหมากมีปริมาณมากที่สุด โดยประกอบด้วยลิกนินร้อยละ 34.51 และเฮมิเซลลูโลสร้อยละ 65.39 นอกจากนี้ยังได้มีการนำเอาวัสดุลิกโนเซลลูโลสที่รีเจนเนอเรทได้จากกาบหมากมาเตรียมคาร์บอนโมโนลิทที่มีรูพรุนแบบลำดับชั้นโดยนำมาผสมกับสารละลายริโซซินอล-ฟอร์มาลดีไฮด์ (อาร์-เอฟ) ได้เป็นเจลผสม อาร์-เอฟ-ลิกโนเซลลูโลส แล้วนำไปผ่านกระบวนการคาร์บอนไนเซชัน ในการศึกษาได้มีการเปรียบเทียบคุณสมบัติและโครงสร้างรูพรุนของคาร์บอนโมโนลิทที่ได้มาจากการคาร์บอนไนเซชัน อาร์-เอฟ-ลิกโนเซลลูโลส เจล กับ อาร์-เอฟ-ลิกนิน-เฮมิเซลลูโลส เจล (โดยใช้อัตราส่วนลิกนินและเฮมิเซลลูโลสในปริมาณเท่ากันกับที่มีอยู่ในวัสดุลิกโนเซลลูโลส) นอกจากนี้ยังได้มีการเตรียมคาร์บอนโมโนลิทที่ได้จากการคาร์บอนไนเซชัน อาร์-เอฟ-ลิกนิน เจล และ อาร์-เอฟ-เฮมิเซลลูโลส เจล เพื่อนำมาเป็นข้อมูลในการเปรียบเทียบอีกด้วย โดยในงานวิจัยนี้ได้มีการศึกษาผลของปริมาณสารละลายลิกนิน เฮมิเซลลูโลสและลิกโนเซลลูโลสที่เติมเข้าไปผสมกับสารละลาย อาร์-เอฟ และค่าพีเอชในช่วงแรกของการเตรียมสารละลายผสม ที่มีผลต่อโครงสร้างรูพรุนของคาร์บอนโมโนลิทที่เตรียมได้ ผลการศึกษาพบว่า เมื่อมีการเติมสารละลายลิกนินเข้าไปในปริมาณที่เหมาะสมจะทำให้ค่าพื้นที่ผิวและปริมาตรรูพรุนรวมของคาร์บอนโมโนลิทเพิ่มขึ้นจาก 333.23 ตารางเมตรต่อกรัม ไปเป็น 482.00 ตารางเมตรต่อกรัมและ 0.22 ลูกบาศก์เมตรต่อกรัม ไปเป็น 0.98 ลูกบาศก์เมตรต่อกรัม ตามลำดับ และมีผลอย่างมากต่อโครงสร้างรูพรุนของคาร์บอนโมโนลิทที่เตรียมได้ โดยสามารถเปลี่ยนโครงสร้างรูพรุนของคาร์บอนที่ได้จากการคาร์บอนไนเซชัน อาร์-เอฟ เจล เพียงอย่างเดียวจากเดิมที่มีโครงสร้างรูพรุนแบบลำดับชั้นของไมโครพอร์บนแมคโครพอร์ไปเป็นคาร์บอนที่มีโครงสร้างรูพรุนแบบลำดับชั้นของเมโซพอร์บนแมคโครพอร์ นอกจากนี้ยังพบอีกว่าค่าพีเอชเริ่มต้นมีผลต่อการเกิดปฏิกิริยาระหว่างลิกนินกับอาร์-เอฟ และมีผลต่อขนาดเส้นผ่านศูนย์กลางของอนุภาคในโครงสร้างของคาร์บอนโมโนลิทด้วย ซึ่งจากการเตรียมคาร์บอนโมโนลิทด้วยวิธีนี้ พบว่ามีความง่ายในการปรับขนาดโครงสร้างรูพรุนของคาร์บอนโมโนลิทเมื่อเทียบกับวิธีการเตรียมด้วยวิธีอื่นๆ เช่น การลอกแบบโครงสร้างรูพรุนแบบลำดับชั้นจากวัสดุอินทรีย์ที่ใช้เป็นเทมเพลต ดังนั้นในงานวิจัยนี้จึงได้นำเสนอวิธีการเตรียมคาร์บอนโมโนลิทที่มีโครงสร้างรูพรุนแบบลำดับชั้นแบบใหม่โดยใช้วัสดุจากธรรมชาติที่มีราคาถูกมาใช้เป็นวัสดุตั้งต้นในการเตรียมคาร์บอนโมโนลิทร่วมกับริโซซินอล-ฟอร์มาลดีไฮด์

ภาควิชา.....วิศวกรรมเคมี..... ลายมือชื่อนิสิต.....  
 สาขาวิชา.....วิศวกรรมเคมี..... ลายมือชื่อ อ.ที่ปรึกษาวิทยานิพนธ์หลัก.....  
 ปีการศึกษา.....2554..... ลายมือชื่อ อ.ที่ปรึกษาวิทยานิพนธ์ร่วม.....

# # 5270468121 : MAJOR CHEMICAL ENGINEERING

KEYWORDS : LIGNOCELLULOSIC MATERIALS / RF GEL / CARBON MONOLITH

RITTIKRAINAMMOONSIN: CARBON MONOLITH FROM RF GELS AND LIGNOCELLULOSIC MATERIALS FROM AGRICULTURAL WASTES. ADVISOR: ASST. PROF. NATTAPORN TONANON, D.Eng, CO-ADVISOR: ADISAK SIYASUKH, D.Eng, 72 pp.

In this work, the dissolution and regeneration of lignocellulosic residues from agricultural wastes have been studied. First, the optimal condition of a solvent (NaOH/H<sub>2</sub>O<sub>2</sub>) for dissolving lignocellulosic residues (rice straw, kapok, luffa and betel palm) has been investigated. Furthermore, all lignocellulosic solutions are regenerated with 2 M H<sub>2</sub>SO<sub>4</sub>. The regeneration of the lignocellulosic solution from betel palm fiber yields the most lignocellulosic material (LCM). The fractions of the obtained lignocellulosic material are 34.51% of lignin and 65.39% of hemicelluloses. Besides, the lignocellulosic material from betel palm fiber is used to prepare carbon gels by mixing with resorcinol-formaldehyde (RF) and the carbon monoliths are obtained by carbonization with N<sub>2</sub>. This work focuses on the effect of lignin, hemicelluloses and lignocellulosic material as well as the initial pH of mixed gel solutions on porous properties and pore structure of carbon monolith. The comparison of the porous properties and pore structure of carbon monolith prepared from RF-lignocellulosic material gels (C-LCM) and RF-lignin-hemicellulose gels (C-LH) is investigated. Moreover, carbon monoliths prepared from RF-lignin gels (C-L) and RF-hemicellulose gels (C-H) have also been studied. The nitrogen adsorption-desorption results show that addition of lignin can lead to increasing S<sub>BET</sub> and total pore volume of carbon monoliths (from 333 m<sup>2</sup>/g to 482 m<sup>2</sup>/g and from 0.23 m<sup>3</sup>/g to 0.98 m<sup>3</sup>/g, respectively). In addition, the porous structure of carbon monolith prepared from RF can be varied from microporous to mesoporous structure when lignin is added to RF (for C-L 4:1). Furthermore, it was found that the initial pH has an effect on cross-linking between lignin and RF as well as the diameter of the nodules on the structure of carbon monolith. This meso-/microporous carbon monolith preparation is more convenient than other methods such as using a hard template of inorganic material and etc. Hence, this work will provide a promising way to use natural resources as a raw material to prepare the hierarchical carbon monoliths.

Department.....Chemical Engineering..... Student's Signature .....

Field of Study.....Chemical Engineering..... Advisor's Signature .....

Academic Year...2011..... Co-advisor's Signature .....

## ACKNOWLEDGEMENTS

I would like to express my deepest appreciation to my advisor, Assistant Professor Nattaporn Tonanon, D.Eng, for her constant supervision, encourage, and kindly support throughout the course of this thesis. Without her sincere help and enlightening advices, this work must not be achieved.

I would like to express my gratitude to my co-advisors, Adisak Siyasukh, D.Eng for his great advices and useful comments throughout all experiment in this research.

I would like to acknowledge Apinan Soottitantawat, Ph.D, Associate Professor Mongkol Sukwattanasinitt, Ph.D, and Sirapat Pratontep, Ph.D, for their useful comments and participation as the thesis committees.

I would like to acknowledge Mr. Wannadara Intrarapanya, Laboratory Staff at Department of Chemical Engineering, Chulalongkorn University, for his supporting on technical assistance.

I would like to thanks all friends and staffs in Center of Excellence in Particle Technology (CEPT), at Department of Chemical Engineering, Chulalongkorn University, for their supporting and kind assistance.

This work has been fully supported by Chulalongkorn University Centenary Academic Development Project.

Finally, I would like to close with my deepest appreciation to my family for their understanding, assistance, constant encouragement and warmhearted support throughout my entire education.

# CONTENTS

|                                                         | <b>PAGE</b> |
|---------------------------------------------------------|-------------|
| <b>ABSTRACT (THAI)</b> .....                            | iv          |
| <b>ABSTRACT (ENGLISH)</b> .....                         | v           |
| <b>ACKNOWLEDGEMENTS</b> .....                           | vi          |
| <b>CONTENTS</b> .....                                   | vii         |
| <b>LIST OF TABLES</b> .....                             | x           |
| <b>LIST OF FIGURES</b> .....                            | xi          |
| <b>NOMENCLATURES</b> .....                              | xiii        |
| <br>                                                    |             |
| <b>CHAPTER I</b>                                        |             |
| <b>INTRODUCTION</b> .....                               | 1           |
| 1.1 Introduction.....                                   | 1           |
| 1.2 Objective of this research.....                     | 2           |
| 1.3 Scope of work.....                                  | 3           |
| <br>                                                    |             |
| <b>CHAPTER II THEORETICAL BACKGROUND AND LITERATURE</b> |             |
| <b>REVIEWS</b> .....                                    | 5           |
| 2.1 Lignocellulosic biomass materials.....              | 5           |
| 2.1.1 Chemical structure.....                           | 5           |
| 2.1.1.1 Cellulose.....                                  | 6           |
| 2.1.1.2 Hemicellulose.....                              | 7           |
| 2.1.1.3 Lignin.....                                     | 7           |
| 2.2 Carbon nanostructure.....                           | 10          |
| 2.2.1 Activated carbon.....                             | 11          |
| 2.3 Nitrogen adsorption-desorption isotherm.....        | 13          |
| 2.4 Hierarchical porous carbon monolith.....            | 16          |
| 2.4.1 Resorcinol-formaldehyde gels.....                 | 16          |
| 2.4.2 Synthesis of RF gels and carbon gels.....         | 16          |
| 2.5 Review papers.....                                  | 21          |

|                                                                                                                                  | <b>PAGE</b> |
|----------------------------------------------------------------------------------------------------------------------------------|-------------|
| <b>CHAPTER III EXPERIMENTAL PROCEDURE</b> .....                                                                                  | 24          |
| 3.1 Chemical reagents.....                                                                                                       | 24          |
| 3.2 Equipments.....                                                                                                              | 25          |
| 3.2.1 Basic equipments.....                                                                                                      | 25          |
| 3.2.2 Horizontal furnace.....                                                                                                    | 25          |
| 3.3 Characterizations.....                                                                                                       | 26          |
| 3.4 Experimental procedures.....                                                                                                 | 27          |
| 3.4.1 Dissolution and regeneration of lignocellulosic residues....                                                               | 27          |
| 3.4.1.1 Characterization of lignocellulosic materials<br>(LCM).....                                                              | 28          |
| 3.4.2 Preparation of hierarchical porous carbon monolith.....                                                                    | 29          |
| 3.4.2.1 Preparation of RF gels.....                                                                                              | 30          |
| 3.4.2.2 Preparation of RF gels mixed lignin (L),<br>hemicellulose (H), lignocellulosic materials<br>(LCM).....                   | 30          |
| 3.4.2.3 Carbonization of RF monolith gel with N <sub>2</sub> .....                                                               | 31          |
| 3.4.2.4 Characterization.....                                                                                                    | 31          |
| <b>CHAPTER IV RESULTS AND DISCUSSIONS</b> .....                                                                                  | 32          |
| 4.1 Dissolution and regeneration of lignocellulosic residues.....                                                                | 32          |
| 4.2 Composition of lignocellulosic materials regenerated from betel<br>palm.....                                                 | 33          |
| 4.3 Characterization of carbon monolith.....                                                                                     | 33          |
| 4.3.1 The influence of lignin (L) on porous properties and<br>chemical structure of carbon monolith.....                         | 34          |
| 4.3.2 The influence of hemicellulose (H) on porous properties<br>and chemical structure of carbon monolith.....                  | 43          |
| 4.3.3 The influence of lignocellulosic materials (LCM) on<br>porous properties and chemical structure of carbon<br>monolith..... | 46          |



|                                                                                                | <b>PAGE</b> |
|------------------------------------------------------------------------------------------------|-------------|
| <b>CHAPTER V CONCLUSIONS</b> .....                                                             | 51          |
| 5.1 The optimal condition for dissolution and regeneration of<br>lignocellulosic residues..... | 51          |
| 5.2 The porous properties and chemical structure of carbon monolith....                        | 51          |
| <b>REFERENCES</b> .....                                                                        | 54          |
| <b>APPENDIX</b> .....                                                                          | 58          |
| <b>BIOGRAPHY</b> .....                                                                         | 72          |

## LIST OF TABLES

|                                                                                                              | <b>PAGE</b> |
|--------------------------------------------------------------------------------------------------------------|-------------|
| <b>Table 2.1</b> Features of adsorption isotherms.....                                                       | 15          |
| <b>Table 2.2</b> IUPAC classification of pores.....                                                          | 15          |
| <b>Table 2.3</b> Solvent-exchange and drying: Effects of various factors on<br>the resulting properties..... | 18          |
| <b>Table 3.1</b> List of chemical reagents in this research.....                                             | 24          |
| <b>Table 4.1</b> The compositional data of lignocellulosic materials.....                                    | 33          |
| <b>Table 4.2</b> Synthesis conditions of carbon monolith gels.....                                           | 34          |
| <b>Table 4.3</b> Porosity of C-RF and C-L.....                                                               | 37          |
| <b>Table 4.4</b> Infrared spectrum peaks for an interpretation of surface<br>functional groups.....          | 39          |
| <b>Table 4.5</b> The main functional groups of lignin and hemicelluloses.....                                | 41          |
| <b>Table 4.6</b> Porosity of C-H.....                                                                        | 44          |
| <b>Table 4.7</b> Porosity of C-LCM and C-LH.....                                                             | 48          |

## LIST OF FIGURES

|                    |                                                                                                               | PAGE |
|--------------------|---------------------------------------------------------------------------------------------------------------|------|
| <b>Figure 1.1</b>  | Schematic diagrams of the scopes in this work.....                                                            | 3    |
| <b>Figure 2.1</b>  | The component of lignocellulosic biomass.....                                                                 | 5    |
| <b>Figure 2.2</b>  | The chemical structure of cellulose.....                                                                      | 6    |
| <b>Figure 2.3</b>  | The sugar component of hemicelluloses.....                                                                    | 7    |
| <b>Figure 2.4</b>  | The chemical structure of lignin.....                                                                         | 8    |
| <b>Figure 2.5</b>  | The monolignols of lignin.....                                                                                | 8    |
| <b>Figure 2.6</b>  | The major types of structural element in lignin.....                                                          | 9    |
| <b>Figure 2.7</b>  | Carbon nanostructure.....                                                                                     | 11   |
| <b>Figure 2.8</b>  | Activated carbon.....                                                                                         | 12   |
| <b>Figure 2.9</b>  | IUPAC classification of adsorption isotherms.....                                                             | 13   |
| <b>Figure 2.10</b> | Activated carbon adsorbs gases and chemicals.....                                                             | 14   |
| <b>Figure 2.11</b> | Classification of pore.....                                                                                   | 15   |
| <b>Figure 2.12</b> | Reaction mechanism of the sol-gel polymerization of resorcinol<br>with formaldehyde.....                      | 17   |
| <b>Figure 2.13</b> | Schematic diagram of the sol-gel polycondensation of a RF<br>solution.....                                    | 17   |
| <b>Figure 2.14</b> | The effect of drying on the structure of RF gels.....                                                         | 19   |
| <b>Figure 3.1</b>  | Schematic diagram of the quartz tube furnace used in this<br>work.....                                        | 26   |
| <b>Figure 3.2</b>  | Dissolution and regeneration of lignocellulosic residues.....                                                 | 27   |
| <b>Figure 3.3a</b> | Rice straw.....                                                                                               | 28   |
| <b>Figure 3.3b</b> | Kapok.....                                                                                                    | 28   |
| <b>Figure 3.3c</b> | Luffa.....                                                                                                    | 28   |
| <b>Figure 3.3d</b> | Betel palm fiber.....                                                                                         | 28   |
| <b>Figure 3.4</b>  | Preparation of carbon monolith diagrams.....                                                                  | 29   |
| <b>Figure 4.1</b>  | Solubility of lignocellulosic residues in NaOH (8wt%)<br>/H <sub>2</sub> O <sub>2</sub> (10wt%) at 80 °C..... | 32   |

|                                                                                                            | <b>PAGE</b> |
|------------------------------------------------------------------------------------------------------------|-------------|
| <b>Figure 4.2a</b> SEM images of porous structure of carbon monolith prepared from RF gels.....            | 35          |
| <b>Figure 4.2b</b> SEM images of porous structure of carbon monolith prepared from RF/L (4:1) gels.....    | 35          |
| <b>Figure 4.2c</b> SEM images of porous structure of carbon monolith prepared from RF/L (1:1) gels.....    | 35          |
| <b>Figure 4.3</b> N <sub>2</sub> adsorption –desorption isotherm of C-RF.....                              | 36          |
| <b>Figure 4.4</b> N <sub>2</sub> adsorption –desorption isotherm of C-L (4:1).....                         | 36          |
| <b>Figure 4.5</b> N <sub>2</sub> adsorption –desorption isotherm of C-L (1:1).....                         | 37          |
| <b>Figure 4.6a</b> FTIR spectra of the C (RF).....                                                         | 42          |
| <b>Figure 4.6b</b> FTIR spectra of the C-L (1:1).....                                                      | 42          |
| <b>Figure 4.6c</b> FTIR spectra of the C-L (4:1).....                                                      | 42          |
| <b>Figure 4.6d</b> FTIR spectra of the lignin carbonized at 500 °C.....                                    | 42          |
| <b>Figure 4.7a</b> SEM images of porous structure of carbon monolith prepared from RF/H (4:1) gels.....    | 43          |
| <b>Figure 4.7b</b> SEM images of porous structure of carbon monolith prepared from RF/H (1:1) gels.....    | 43          |
| <b>Figure 4.8a</b> N <sub>2</sub> adsorption –desorption isotherm of C-H (4:1).....                        | 44          |
| <b>Figure 4.8b</b> N <sub>2</sub> adsorption –desorption isotherm of C-H (1:1).....                        | 44          |
| <b>Figure 4.9a</b> FTIR spectra of the C (RF) .....                                                        | 45          |
| <b>Figure 4.9b</b> FTIR spectra of the C-H (1:1).....                                                      | 45          |
| <b>Figure 4.9c</b> FTIR spectra of the C-H (4:1).....                                                      | 45          |
| <b>Figure 4.9d</b> FTIR spectra of the hemicellulose carbonized at 500 °C.....                             | 45          |
| <b>Figure 4.10a</b> SEM images of porous structure of carbon monolith prepared from RF/LCM (4:1) gels..... | 46          |
| <b>Figure 4.10b</b> SEM images of porous structure of carbon monolith prepared from RF/LCM (1:1) gels..... | 46          |

|                                                                                                           | <b>PAGE</b> |
|-----------------------------------------------------------------------------------------------------------|-------------|
| <b>Figure 4.10c</b> SEM images of porous structure of carbon monolith prepared from RF/LH (4:1) gels..... | 46          |
| <b>Figure 4.10d</b> SEM images of porous structure of carbon monolith prepared from RF/LH (1:1) gels..... | 46          |
| <b>Figure 4.11a</b> N <sub>2</sub> adsorption –desorption isotherm of C-LCM, C-LH (4:1).....              | 47          |
| <b>Figure 4.11b</b> N <sub>2</sub> adsorption –desorption isotherm of C-LCM, C-LH (1:1).....              | 47          |
| <b>Figure 4.12a</b> FTIR spectra of the C (RF).....                                                       | 49          |
| <b>Figure 4.12b</b> FTIR spectra of the C-LCM (1:1).....                                                  | 49          |
| <b>Figure 4.12c</b> FTIR spectra of the C-LCM (4:1).....                                                  | 49          |
| <b>Figure 4.12d</b> FTIR spectra of the lignin carbonized at 500 °C.....                                  | 49          |
| <b>Figure 4.12e</b> FTIR spectra of the hemicellulose carbonized at 500 °C.....                           | 49          |
| <b>Figure 4.13a</b> FTIR spectra of the C (RF).....                                                       | 49          |
| <b>Figure 4.13b</b> FTIR spectra of the C-LH (1:1).....                                                   | 49          |
| <b>Figure 4.13c</b> FTIR spectra of the C-LH (4:1).....                                                   | 49          |
| <b>Figure 4.13d</b> FTIR spectra of the lignin carbonized at 500 °C.....                                  | 49          |
| <b>Figure 4.13e</b> FTIR spectra of the hemicellulose carbonized at 500 °C.....                           | 49          |

## NOMENCLATURES

|                    |                                                                     |
|--------------------|---------------------------------------------------------------------|
| C                  | = Carbon                                                            |
| C/W                | = Mole to volume ratio of catalyst to water [mol/m <sup>3</sup> ]   |
| DP                 | = Degree of polymerization                                          |
| <i>et al.</i>      | = et alibi (latin), and others                                      |
| F                  | = Formaldehyde                                                      |
| FT-IR              | = Fourier Transform Infrared Spectroscopy                           |
| H                  | = Hemicellulose                                                     |
| HPLC               | = High performance liquid chromatography                            |
| L                  | = Lignin                                                            |
| LCM                | = Lignocellulosic materials                                         |
| LH                 | = Lignin/Hemicellulose                                              |
| M                  | = Molar [mol/liter]                                                 |
| Mw                 | = Molecular weight                                                  |
| nm                 | = Nanometer                                                         |
| N <sub>2</sub>     | = Nitrogen gas                                                      |
| P/P <sub>0</sub>   | = Relative pressure of N <sub>2</sub> gas [-]                       |
| R                  | = Resorcinol                                                        |
| R/F                | = Molar ratio of resorcinol to formaldehyde [-]                     |
| R/W                | = Molar ratio of resorcinol to de-ionized water [-]                 |
| RF                 | = Resorcinol-formaldehyde gel                                       |
| S                  | = Dissolution degree                                                |
| S <sub>BET</sub>   | = Specific surface area determined by BET model [m <sup>2</sup> /g] |
| SEM                | = Scanning electron microscopy                                      |
| T                  | = Tanin                                                             |
| UV-VIS             | = Ultraviolet-visible spectroscopy                                  |
| V                  | = Adsorption volume at STP of N <sub>2</sub> [cm <sup>3</sup> /g]   |
| V <sub>meso</sub>  | = Mesopore volume [cm <sup>3</sup> /g]                              |
| V <sub>micro</sub> | = Micropore volume [cm <sup>3</sup> /g]                             |
| v/v                | = Volume by volume                                                  |

|                |                                                   |
|----------------|---------------------------------------------------|
| W              | = De-ionized water                                |
| W <sub>o</sub> | = original weight of the lignocellulosic residues |
| W <sub>r</sub> | = weight of undissolved lignocellulosic residues  |
| w/w            | = Weight by weigh                                 |
| XRD            | = X-ray diffractometer                            |

# CHAPTER I

## INTRODUCTION

### 1.1 Introduction

Most agricultural wastes are composed of cellulose, hemicelluloses and lignin (called lignocellulosic wastes). They are comprised of different percentages of cellulose, hemicelluloses and lignin. Most of them can be largely found in agricultural industry such as rice straw, corn stover, bagasse and etc. Thailand as an agricultural base country, lignocellulosic wastes from various kinds of crop have not fully utilized. Extracting some components of lignocellulosic wastes and using them in various applications are the promising way for adding value of lignocellulosic wastes. For many years, the dissolution of lignocellulosic wastes has attracted the attention of research because they are the most abundant organic resources on earth. Only lignin and hemicelluloses can be dissolved at high temperature [1-2], but cellulose that is the main component of lignocellulosic wastes is not able to dissolved because of its strong crystalline structure. Both lignin and hemicellulose can be depolymerized to produce starting materials for phenolic resin, epoxy and furan resin production [3].

Porous carbon materials prepared by polycondensation of resorcinol and formaldehyde in a solvent followed by drying and carbonization have been extensively studied for many years [4-6]. Various carbon materials whose texture depends on the nature of the precursors, the gelation conditions and the drying method can be obtained [7-12]. Porous carbons have a variety of potential and current applications, including in gas separation and absorption, enzyme immobilization for high-throughput bioreactor catalyst, HPLC monolithic column for high speed separation, membrane emulsification and catalyst supports. For the past few years, there have been many studies investigating the unique properties and applications of carbon porous materials. Furthermore, several efforts have been made to simplify the processing and to exploit cheap raw materials from biological resources [13]. Because of its phenolic molecules, lignin and hemicellulose can react and polymerise with formaldehyde and also such compounds are cheap, non-toxic and ecologic. The



corresponding molecules comprise aromatic rings bearing hydroxyl groups, they present reactivity rather similar to that of resorcinol or phenol [14], and may thus be a very valuable substitute to such more expensive molecules from petrochemicals. Some of the porous materials can exhibit some unique properties, such as a high specific surface area, a pronounced mesoporosity and a structure composed of uniform-size nanoparticles.

In this research, the dissolution and regeneration of lignocellulosic waste are studied. Lignocellulosic materials obtained from regenerating lignocellulosic solutions are used as a starting material together with resorcinol and formaldehyde in preparing hierarchical porous carbon monoliths. The comparisons between characteristics of the hierarchical porous carbon monoliths prepared from lignocellulosic material and the commercial ones are investigated. This work will remarkably introduce an interesting way on preparing the hierarchical porous carbon monoliths in a simple way.

## **1.2 Objectives of this research**

The dissolution and regeneration of lignocellulosic residues are studied by using rice straw, kapok, luffa and betel palm fiber as raw materials. Lignocellulosic materials are mixed with resorcinol-formaldehyde solutions to prepare a mixed gel, and follow by carbonization in a horizontal furnace.

The objectives in this work can be separated into three parts as follows:

1. To study on the dissolution and regeneration of lignocellulosic residues.
2. To study on the preparation of hierarchical porous carbon monoliths by using resorcinol, formaldehyde and lignocellulosic materials as a starting material.
3. To study on the properties of hierarchical porous carbon monoliths prepared from lignocellulosic materials and the commercial ones.

### 1.3 Scopes of work

All experiments in this research are performed in laboratory scale. The scopes for study in this work are divided into two main sections as shown in Figure 1.1.

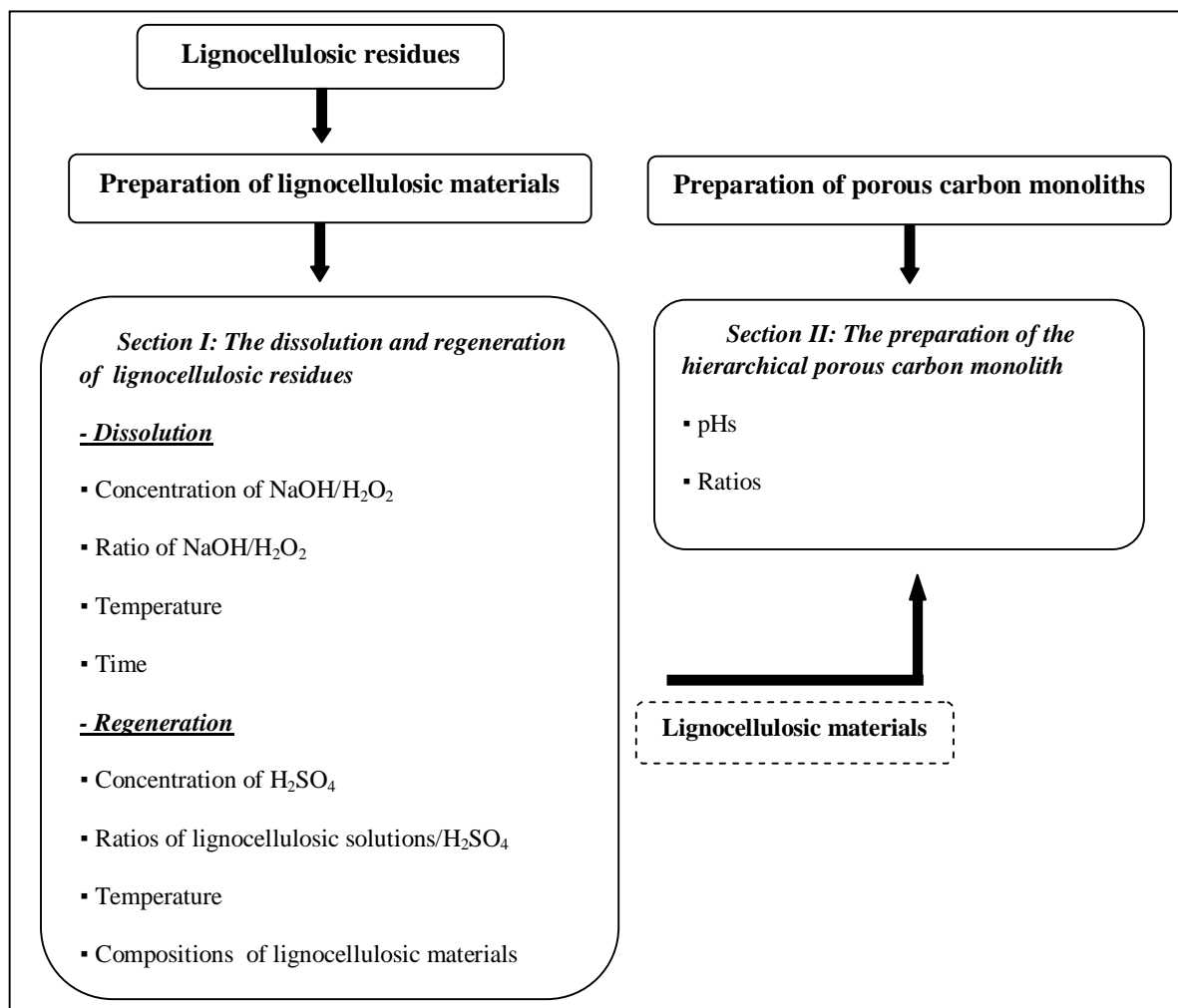


Figure 1.1 Schematic diagrams of the scopes in this work

### Section I The dissolution and regeneration of betel palm fiber

In this section, rice straw, kapok, luffa and betel palm fiber are used as raw materials to find the optimal condition for the dissolution of lignocellulosic residues in NaOH/H<sub>2</sub>O<sub>2</sub> at high temperature.

The primary conditions for finding the optimal condition are studied as follows:

- Concentrations
  - NaOH is studied in the range of 2-10 %wt.
  - H<sub>2</sub>O<sub>2</sub> is studied in the range of 2.5-20 %wt.
- Temperature
- Time
- Ratios of NaOH/H<sub>2</sub>O<sub>2</sub>

Moreover, the regeneration of lignocellulosic solutions is investigated. Sulfuric acid (H<sub>2</sub>SO<sub>4</sub>) is used as a coagulant by varying the concentration at 0.5, 1, 1.5 and 2 M and the temperature bath is performed in the range of 30-50 °C. The ratios between coagulants and solutions are also investigated at 1:1, 1:2, 1:4 and 1:8. The compositions of lignocellulosic materials regenerated from the solutions are determined by autohydrolysis method.

### Section II The preparation of the hierarchical porous carbon monoliths

In this part, lignocellulosic materials are dissolved and mixed with the resorcinol (R)-formaldehyde (F) solution during preparation for synthesis of RF monolith gels, and subsequently dried in hot air oven. The synthesis variables are focused on the initial pH value of mixed solutions in the range of 1.5-7.0, and the ratios of RF:lignocellulosic solutions are studied at 4:1 and 1:1. All of the monolith gels are carbonized with a horizontal furnace reactor to obtain the hierarchical porous carbon monoliths. The porous properties of the hierarchical porous carbon monoliths are investigated.

## CHAPTER II

### THEORETICAL BACKGROUND AND LITERATURE REVIEWS

#### 2.1 Lignocellulosic biomass materials

Lignocellulosic biomass is the most abundant material in the world. Its sources range from trees to agricultural residues. Long ago, these materials were used as firewood, building materials and animal food. Nowadays, lignocellulosic materials are not just used in their old ways, their applications have expanded into the fiber level as in pulp and paper products. In some cases, the use of lignocellulose is proceeding to the level of the chemical component itself. For example, cellulose, which is a major chemical constituent of lignocellulosic materials can be used for fibers in the textile industry; while lignin is used as an adhesive component in the composite industry.

##### 2.1.1 Chemical structure

The chemical components of lignocellulosic biomass can be divided into four major components. They are cellulose, hemicelluloses, lignin and extractives. Generally, the first three components have high molecular weights and contribute much mass, while the latter component is of small molecular size, and it is available in little quantity. Based on weight percentage, cellulose and hemicelluloses are higher in hardwoods compared to softwoods and wheat straw, while softwoods have higher lignin content. Wheat straw has a high percentage of extractives.

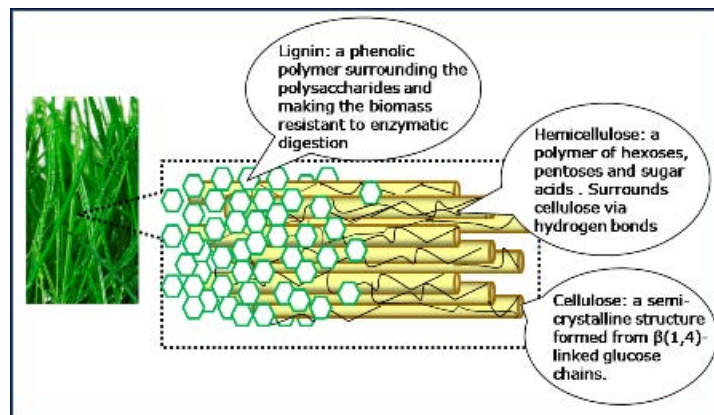


Figure 2.1: The component of lignocellulosic biomass [15]

### 2.1.1.1 Cellulose

The amount of cellulose, in lignocellulosic systems, can vary depending on the species or age of the plant. Cellulose is a hydrophilic glucan polymer consisting of a linear chain of 1,4- $\beta$  anhydroglucose units, which contain alcoholic hydroxyl groups. These hydroxyl groups form intermolecular and intramolecular hydrogen bonds with the macromolecule itself and also with other cellulose macromolecules or polar molecules.

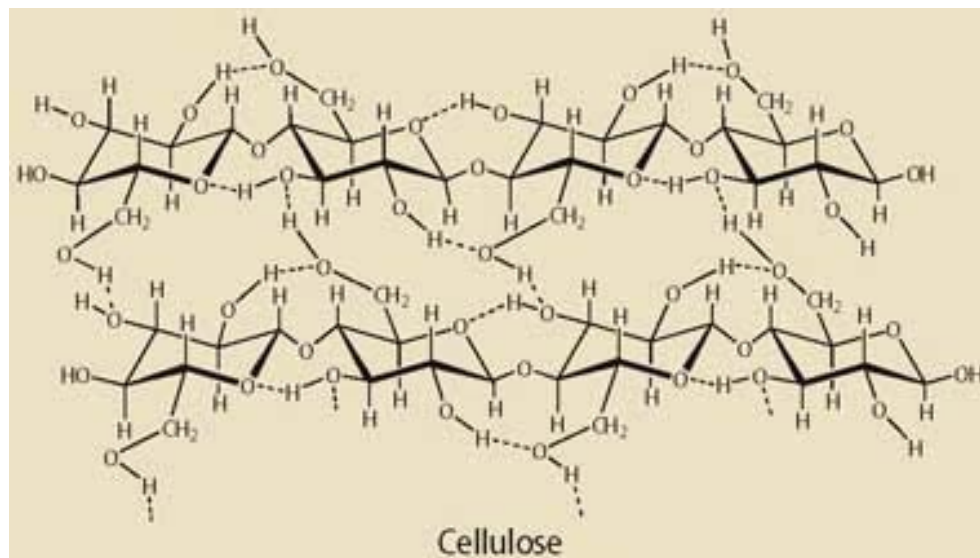


Figure 2.2: The chemical structure of cellulose [15]

Therefore, all natural fibers are hydrophilic in nature. Although the chemical structure of cellulose from different natural fibers is the same, the degree of polymerization (DP) varies. The mechanical properties of a fiber are significantly dependent on the DP. The degree of polymerization (DP) of native cellulose is in the range of 7,000-15,000. Cellulosic materials present amorphous and crystalline domains. The crystallinity rate depends on the origin of the materials.

### 2.1.1.2 Hemicellulose

Unlike cellulose, hemicelluloses consist of different monosaccharide units. In addition, the polymer chains of hemicelluloses have short branches and are amorphous. Because of the amorphous morphology, hemicelluloses are partially soluble or swellable in water. The backbone of the chains of hemicelluloses can be a homopolymer (generally consisting of single sugar repeat unit) or a heteropolymer (mixture of different sugars). Formulas of the sugar component of hemicelluloses are listed in Figure 2.3. Among the most important sugar of the hemicelluloses component is xylose.

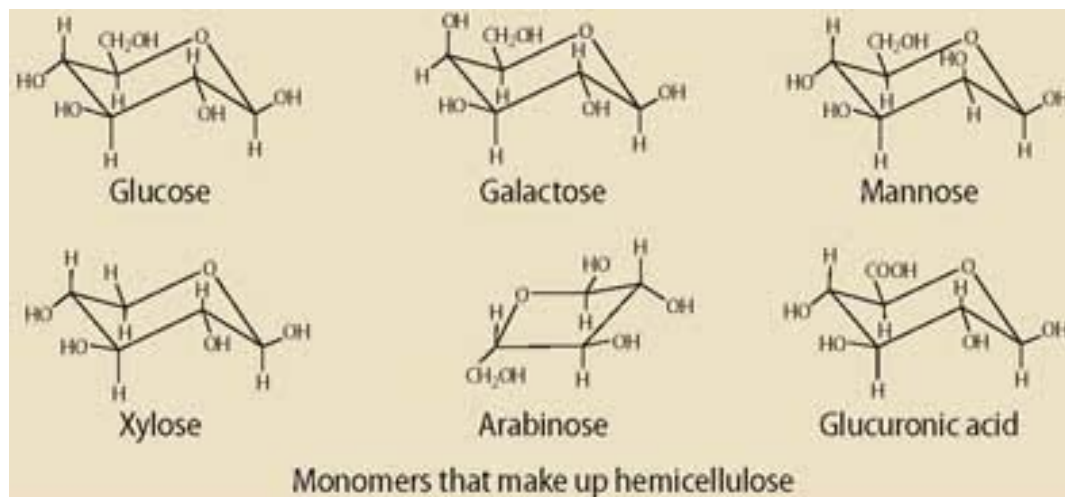


Figure 2.3: The sugar component of hemicelluloses [15]

### 2.1.1.3 Lignin

Lignins are polymeric aromatic constituents. They are traditionally considered to be dehydrogenative polymers from three monolignols: p-coumaryl alcohol, coniferyl alcohol and sinapyl alcohol [16].

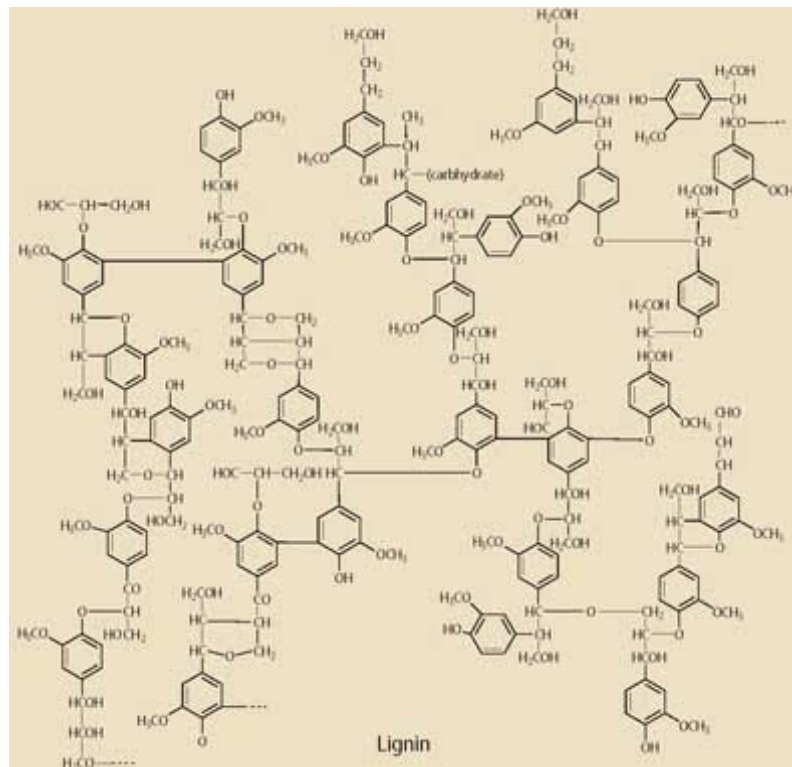


Figure 2.4: The chemical structure of lignin [15]

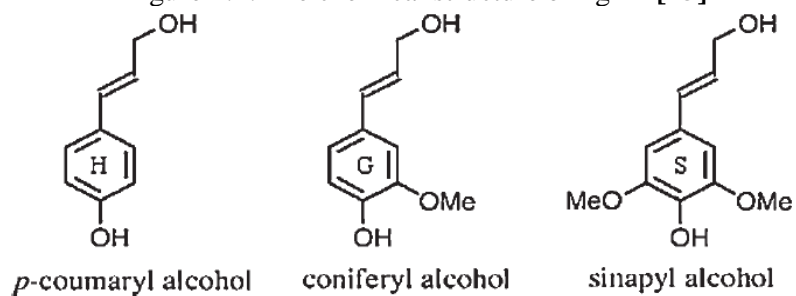


Figure 2.5: The monolignols of lignin [16]

Because of structure complexity there is no uniform knowledge about chemical and physical structure of this polymer and it is possible to consider only chemical lignin models. The predominant linkage is the so-called  $\beta$ -O-4 linkage. About 40-60% of all inter unit linkages in lignin is via ether bond.

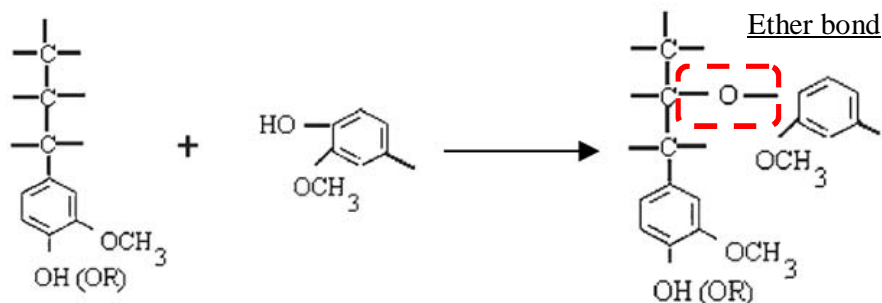


Figure 2.6: The major types of structural element in lignin [16]

The high carbon and low hydrogen content of lignin suggest that it is unsaturated or aromatic in nature. Lignin is characterized by its associated hydroxyl and methoxy groups. The topology of lignin from different sources may be different but it has the same basic composition. Although the exact mode of linkages of lignin with cellulose in lignocellulosic natural fiber is not well known, lignin is believed to be linked with the carbohydrate moiety through two types of linkages, one alkali sensitive and the alkali resistant. The alkali-sensitive linkage forms an ester-type combination between lignin hydroxyls and carboxyls of hemicelluloses uronic acid. The ether-type linkage occurs through the lignin hydroxyls combining with the hydroxyls of cellulose. The lignin, being polyfunctional, exists in combination with more than one neighboring chain molecule of cellulose and/or hemicelluloses, making a cross-linked structure.

Because of its abundant resource, lignocellulosic biomass has been a very active research area during the recent year. Dissolution and regeneration of lignocellulosic biomass are an interesting study to extract lignin and hemicellulose from cellulose. In addition, extracted hemicellulose and lignin can be depolymerized to produce starting materials for phenolic resin, epoxy, and furan resin production.

R. Sun et al. [1] has been first investigated in alkaline peroxide delignification of rye straw. The results showed that treatment of dewaxed and water-extracted rye straw with 2%  $\text{H}_2\text{O}_2$  at pH 11.5 for 12 h at 20-70°C resulted in a dissolution of 52.7-87.8% of the original lignin, and 44.2- 71.9% of the original hemicelluloses,



respectively. The isolated pure lignin fractions contained rather low amounts of neutral sugars, 0.4–1.1%, and had weight-average molecular weights between 2420 and 3480 g mol<sup>-1</sup>. They contained almost equal amounts of noncondensed guaiacyl and syringyl units with fewer *p*-hydroxyphenyl units. The b–O–4 ether bonds together with b–b and b–5 carbon–carbon linkages were found to be present in the lignin structural units. Comparison of these lignin samples indicated that the alkaline peroxide treatment of the straw under the conditions given did not affect the overall structure of lignin.

N. Muhammad *et al.* [17] studied on the dissolution and regeneration of bamboo by using ionic liquids at high temperature (165 °C). It has been observed that only 3-(1-methylimidazolium-3-yl) propane-1-sulfonate (MIM-PS) ionic liquid due to its zwitterions effect has the potential to dissolve biomass. From FIIR spectra of regenerated materials it has been concluded that lignin could be partially removed by ionic liquid treatment. From XRD analysis it has been observed that during dissolution of biomass in ionic liquid the crystallinity of cellulose changed from cellulose I to its amorphous state. From SEM analysis it has been observed that fibrous nature of material disappeared and it was converted into particle nature of materials

## 2.2 Carbon nanostructure

The field of carbon structures was reenergized by the discovery of fullerenes and carbon nanotubes [18]. In addition to generating tremendous interest in the fundamental properties of discrete carbon molecules and nano-objects these nano-structured carbons have found, or are expected to have, numerous commercial applications such as advanced fillers, materials for energy and gas storage, sensors and elements for molecular electronics devices. Two different strategies have been developed for the preparation of engineering carbon materials; one includes pyrolysis of organic precursors (mostly polymeric) under an inert atmosphere to yield large-scale engineering carbons and the other involves physical/chemical vapor deposition techniques that produce well-defined nanostructured carbons. Whereas techniques

from the first group are applicable to large scale production, they offer very limited control over the carbon (nano) structure, techniques from the second group do allow atomic scale precision in control of the nanostructure but they are relatively expensive, have limited yield and require complex equipment.

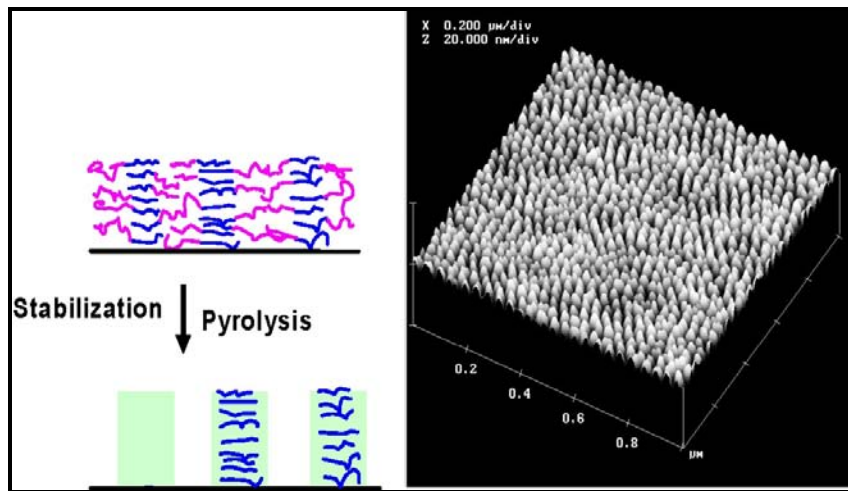


Figure 2.7: Carbon nanostructure [19]

### 2.2.1 Activated carbon

Activated carbon is a form of carbon that has been processed to make it extremely porous and thus to have a very large surface area available for adsorption or chemical reactions.

Due to its high degree of microporosity, just 1 gram of activated carbon has a surface area in excess of  $500 \text{ m}^2$ , as determined typically by nitrogen gas adsorption. Sufficient activation for useful applications may come solely from the high surface area, though further chemical treatment often enhances the absorbing properties of the material. Activated carbon is usually derived from charcoal.



Figure 2.8: Activated carbon

Activated carbon is carbon produced from carbonaceous source materials like nutshells, peat, wood, coir, lignite, coal and petroleum pitch. It can be produced by one of the following processes:

- **Physical reactivation:** The precursor is developed into activated carbons using gases. This is generally done by using one or a combination of the following processes:
  - *Carbonization:* Material with carbon content is pyrolyzed at temperatures in the range 600–900 °C, in absence of oxygen (usually in inert atmosphere with gases like argon or nitrogen)
  - *Activation/Oxidation:* Raw material or carbonized material is exposed to oxidizing atmospheres (carbon monoxide, oxygen, or steam) at temperatures above 250 °C, usually in the temperature range of 600–1200 °C.
- **Chemical activation:** Prior to carbonization, the raw material is impregnated with certain chemicals. The chemical is typically an acid, strong base, or a salt (phosphoric acid, potassium hydroxide, sodium hydroxide, zinc chloride, respectively). Then, the raw material is carbonized at lower temperatures (450–900 °C). It is believed that the carbonization / activation step proceeds simultaneously with the chemical activation. Chemical activation is preferred over physical activation owing to the lower temperatures and shorter time needed for activating material.

### 2.3 Nitrogen adsorption-desorption isotherm

In physical adsorption, adsorption isotherms can be classified as one of 6 types, as shown in the Figure 2.9 below. Table 2.1 shows the types and features, as well as an adsorbent example.

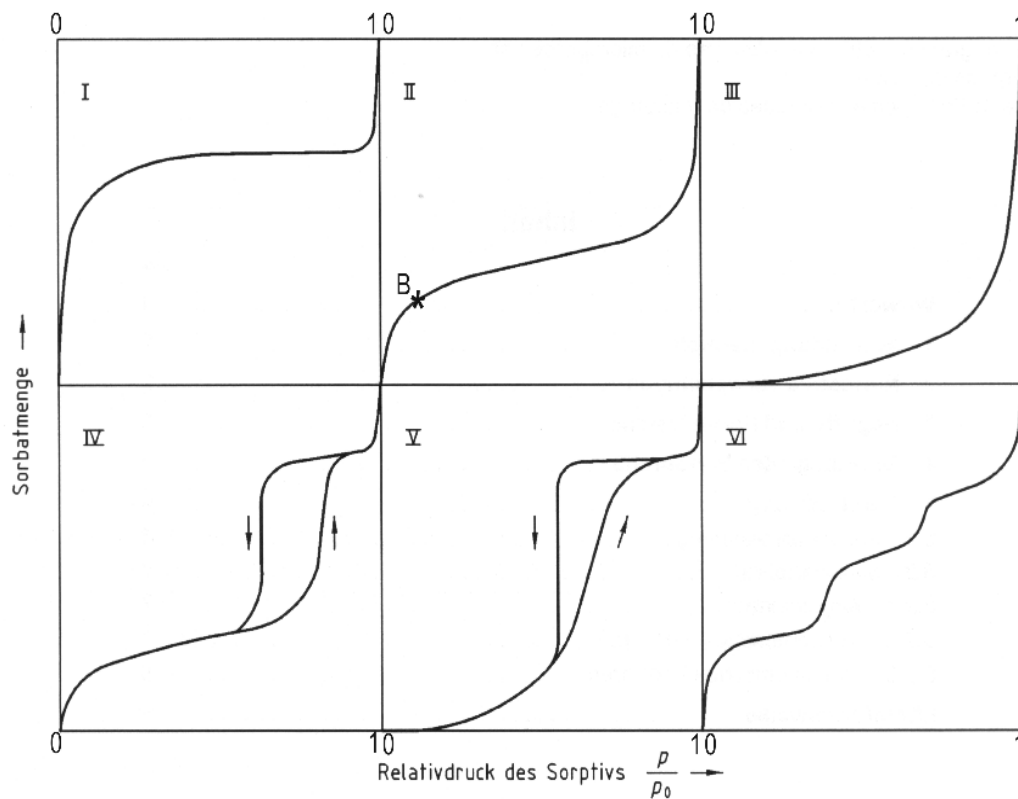


Figure 2.9: IUPAC classification of adsorption isotherms

Type I represents the sorption behavior of micro-porous substances. For low relative pressure a steep increase of isotherms can be seen. In this course the refill with micro-pores is reflected. Afterwards the isotherm proceeds in a horizontal plateau because the surface is covered entirely with the adsorbate. Type II describes a system, which shows multi layer adsorption after reaching the monomolecular adsorbate layer at point B up to the setting in of condensation at  $p/p_0=1$ . Substances without relative large pores (mesopores) show total reversibility at desorption (types I,

II, and III). Mesopores, however, cause a hysteresis (types IV and V). Types III and V shows an increase of the isotherm at higher relative pressures. This is caused by the weak adsorbate-adsorbent interactions. Type VI shows the gradual formation of individual adsorbate layers, which stem from a multimodal pore distribution. The range of validity of the BET model for the determination of the specific surface is in the range of  $0.05 - 0.3 p/p_0$ .

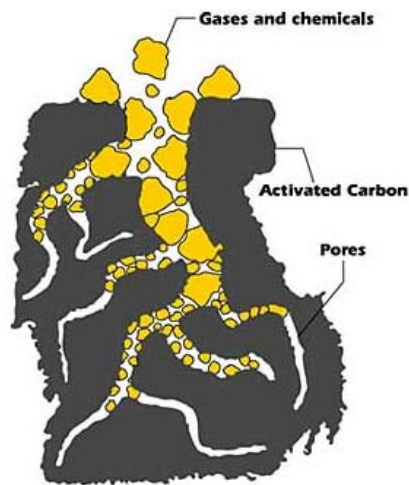


Figure 2.10: Activated carbon adsorbs gases and chemicals

Table 2.1: Features of adsorption isotherms

| Type | Features                                                               |                        | Sample- Adsorptive example   |
|------|------------------------------------------------------------------------|------------------------|------------------------------|
|      | Interaction between sample surface and adsorbate                       | Porosity               |                              |
| I    | Relatively strong                                                      | Micropores             | Activated carbon-Nitrogen    |
| II   | Relatively strong                                                      | Nonporous              | Oxide-Nitrogen               |
| III  | Weak                                                                   | Nonporous              | Carbon-Water vapor           |
| IV   | Relatively strong                                                      | Mesopore               | Silica-Nitrogen              |
| V    | Weak                                                                   | Mesopore/<br>Micropore | Activated carbon-Water vapor |
| VI   | Relatively strong<br>Sample surface has an even distribution of energy | Nonporous              | Graphite-Krypton             |

Size of pores is classified as shown in Table 2.2 below

Table 2.2: IUPAC classification of pores

| <b>Pore</b> | <b>Pore diameter/nm</b> |
|-------------|-------------------------|
| Micropore   | Up to 2                 |
| Mesopore    | 2 to 50                 |
| Macropore   | 50 or up                |

Adsorption isotherms are classified as shown in Table 2.2 based on the strength of the interaction between the sample surface and adsorptive, and the existence or absence of pores. However, some actual samples do not fit into adsorption isotherm types I to VI. These may be measured as mixed types of adsorption isotherm. For example, nitrogen adsorption for a porous sample with large external surface area may generate a compound isotherm resembling types I and II, or types I and IV.

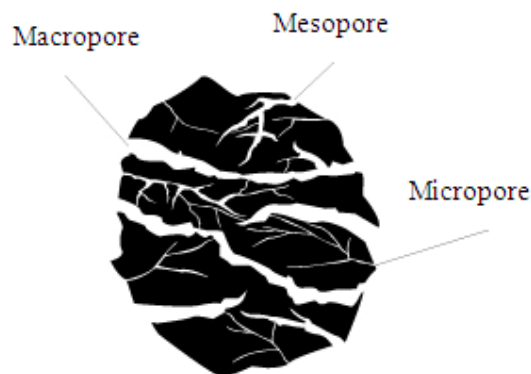


Figure 2.11: Classification of pore

## **2.4 Hierarchical porous carbon monolith**

### **2.4.1 Resorcinol-formaldehyde gels**

The first resorcinol-formaldehyde (RF) gel was produced by Pekala *et al* [20]. RF gels are the porous material classified in family of phenolic resins. They are a convenient precursor of highly porous carbons. Carbon gels were also obtained by carbonization of RF gels in an inert atmosphere. They are attractive and versatile materials which have been suggested for various for electric double-layer supercapacitors or secondary batteries, filling material for HPLC columns, catalyst supports and heat insulator at high temperature [21-25].

### **2.4.2 Synthesis of RF gels and carbon gels**

Highly cross-linked and transparent inorganic hydrogels can be synthesized by sol-gel polycondensation of metal areas alkoxides. RF hydrogels (organic hydrogels) can also be as prepared by sol-gel polycondensation of resorcinol (R) formaldehyde (F) in a slightly basic aqueous solution. The mechanisms of sol-gel polycondensation reaction of RF gels are shown in Figure 2.12 – 2.13.

Carbon gels can be obtained following different procedures, but the preparation mainly consists of three steps: (i) gel synthesis, involving the formation of a three-dimensional polymer in a solvent (gelation), followed by a curing period, (ii) gel drying, where the solvent is removed to obtain an organic gel, and finally (iii) pyrolysis under an inert atmosphere to form the porous carbon material, i.e. the so-called carbon gel [26, 27].

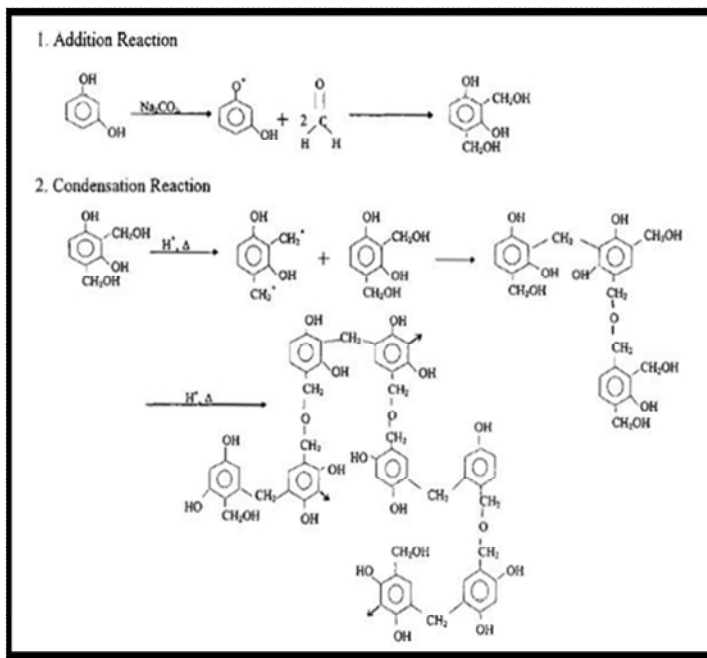


Figure 2.12 Reaction mechanism of the sol-gel polymerization of resorcinol with formaldehyde [4]

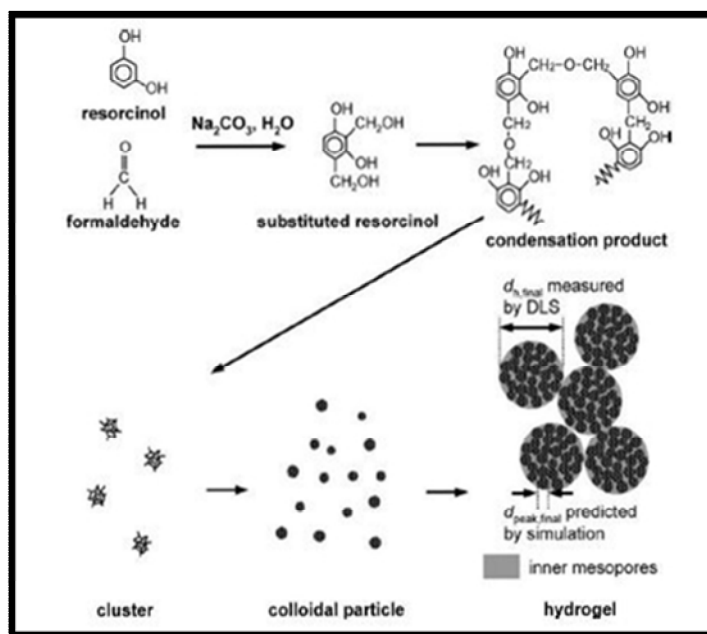


Figure 2.13 Schematic diagram of the sol-gel polycondensation of a RF solution [7-9]



Once the final crosslinked gel is formed, it becomes necessary to remove the aqueous solvent that is possibly used as the reaction medium. The different methods used to remove the solvent have dramatic effects on the properties of the RF organic gels, as outlined in Table 2.3. Typically, the aqueous solvent is replaced with an organic one (e.g., methanol, acetone, isopropanol or amyl acetate).

Table 2.3: Solvent-exchange and drying: Effects of various factors on the resulting properties [28]

| <b>Factor</b>                             | <b>Effect</b>                                                                                                                                                                                                                                                                                                                                                                                 |
|-------------------------------------------|-----------------------------------------------------------------------------------------------------------------------------------------------------------------------------------------------------------------------------------------------------------------------------------------------------------------------------------------------------------------------------------------------|
| Solvent exchange                          | <ul style="list-style-type: none"> <li>-Necessary for supercritical drying with CO<sub>2</sub> or freezing-drying</li> <li>-Facilitates replacement with drying media</li> <li>-Reduction of surface tensions upon subcritical evaporation</li> </ul>                                                                                                                                         |
| Subcritical drying                        | <ul style="list-style-type: none"> <li>-Production of dried dense polymers called “xerogels”</li> <li>-Causes significant shrinkage of especially wide pores</li> <li>-Effects can be significant if gels were synthesized with high mechanical strength</li> <li>-Increase lithium-ion charge and discharge capacities</li> </ul>                                                            |
| Supercritical drying with CO <sub>2</sub> | <ul style="list-style-type: none"> <li>-Production of dried light polymers called “aerogels”</li> <li>-Insignificant shrinkage of pore structure</li> <li>-High surface area, pore volume and, sometime, electrochemical capacitances</li> <li>-Requires high pressures, long times for exchanging solvent with CO<sub>2</sub></li> </ul>                                                     |
| Supercritical drying with acetone         | <ul style="list-style-type: none"> <li>-Like supercritical drying with CO<sub>2</sub>, but with lower pressure</li> <li>-Eliminates necessity for exchanging solvent with CO<sub>2</sub>, shortens processing time significantly</li> <li>-Requires high temperatures to shift acetone to supercritical conditions</li> <li>-May cause partial thermal decomposition of dried gels</li> </ul> |
| Freeze-drying                             | <ul style="list-style-type: none"> <li>-Production of dried light polymers called “cryogels” based on sublimation of frozen solvents</li> <li>-Cryogels mostly mesoporous</li> <li>-Density of solvent must be invariant with freezing</li> </ul>                                                                                                                                             |

T. Yamamoto *et al.* [10] synthesized resorcinol–formaldehyde hydrogels by sol–gel polycondensation of resorcinol with formaldehyde in a slightly basic aqueous solution. RF cryogels, RF xerogels, and RF xerogels (MW gels) were respectively prepared from RF hydrogels by freeze drying, hot air drying, and microwave drying. Carbon cryogels, carbon xerogels and carbon MW gels were subsequently obtained by pyrolyzing RF drygels in an inert atmosphere. Freeze drying and microwave drying were effective to prepare mesoporous RF drygels and carbon gels. RF cryogels and carbon cryogels showed high mesoporosity over wide ranges of the molar ratio of resorcinol to catalyst (R/C) and the ratio of resorcinol to water (R/W) used in sol–gel polycondensation. Although RF xerogels had a few mesopores, carbon xerogels had no mesopores. RF MW gels and carbon MW gels showed mesoporosity if appropriate values of R/C and R/W were selected.

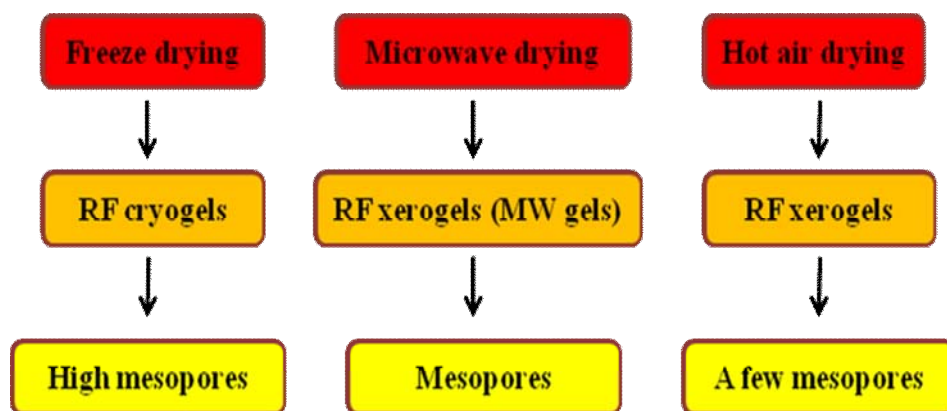


Figure 2.14: The effect of drying on the structure of RF gels

N. Job *et al.* [29] synthesized porous carbon materials by evaporative drying (without any pre-treatment). The pore texture obtained after evaporative drying and pyrolysis is controllable by the pH of the solution. It is possible to define a pH interval that leads to a micro- and mesoporous carbon material. The materials obtained by fixing the pH in this interval exhibit specific surface areas in the range of 550–650 m<sup>2</sup>/g and total void volume varying from 0.40 to 1.40 cm<sup>3</sup>/g after drying and pyrolysis. When the pH is chosen below the lower limit (~5.5 in this study), the

obtained sample is a micro- and macroporous material with poor mechanical strength. When the pH exceeds the upper limit (~6.25 in this study), the obtained material is non-porous.

Mesoporous carbon gels are usually obtained by pyrolyzing resorcinol-formaldehyde (RF) gels, which are synthesized via the sol-gel polycondensation of resorcinol with formaldehyde in a slightly basic aqueous solution followed by drying. However, mesoporous carbon gels cannot be prepared under the conditions of high catalyst concentration or high pH of RF solution even by using supercritical drying or freeze drying.

A. Siyasukh *et al.* [30] improved mesoporosity of carbon cryogels prepared at high C/W or pH by the utilization of ultrasonic in the preparation of RF gel. It is found that the gelation time of RF solution becomes greatly short by ultrasonic irradiation and that ultrasonic can improve mesoporosity of carbon cryogels prepared at high catalyst concentration (C/W). Although the carbon cryogels prepared from C/W = 80 mol/m<sup>3</sup> have no mesopores, the carbon cryogels prepared by ultrasonic irradiation under the same catalyst condition have sharp mesopore size distribution.

A. Siyasukh *et al.* [31] synthesized a hierarchical porous carbon monolith with micropores, mesopores and macropores. In step I, a macroporous interconnected carbon monolith is prepared by ultrasonic irradiation during sol-gel polycondensation. The macropore size of the carbon monoliths increases with decreasing C/W ratios. Higher ultrasonic power leads to broader macropore size distribution, larger mean pore diameter and larger macropore volume of interconnected carbon monolith. In step II, mesopore can be successfully generated on macroporous interconnected carbon monolith by Ca(NO<sub>3</sub>)<sub>2</sub> impregnation and CO<sub>2</sub> activation

## 2.5 Review papers

In the past few years, there have been substantial studies investigating the unique properties and application of porous carbons. Furthermore, many efforts have been made to simplify the processing and to improve the utilization of biological resources as raw materials. Thus, more easily adjustable pore textures may be obtained using a new precursor.

There are many literatures which have been used in studies of the preparation of carbon gels and porous carbons.

F. Chen *et al.* [13] studied on using lignin as a raw material to prepare organic aerogels based upon gelation and supercritical drying in ethanol. The aerogels were prepared from a mixture of the raw materials with lignin (L), resorcinol (R) and formaldehyde (F) followed by a reaction catalyzed by NaOH (C). Aerogels can be prepared under specified experimental conditions, including LRF concentration, LRF ratio, gelation temperature and gelation time. The experimental results showed that the gelation ability of the L-R-F system could be enhanced by increasing the LRF concentration (and the LR/C ratio). The bulk density of the organic aerogels can be controlled by the LRF concentration and the LR/C ratio. The lowest density of organic aerogels was  $0.244 \text{ g/cm}^3$ , which was reached under the conditions of LR/C 25, lignin concentration 50% and LRF concentration 5%. In addition, when the lignin concentration is too high, organic LRF could not be obtained. SEM and TEM micrographs showed that the LRF had an open cell structure with continuous porosity and homogeneous spherical particles. Furthermore, compared to the RF aerogel, the BET surface area, the micropore surface area and the micropore volume of the LRF aerogel was relatively lower, but the average pore width of the LRF aerogel was larger than the RF aerogel. With increasing lignin concentration, the BET surface area and the pore volume of the LRF also became lower, and the pore size distribution ranged widely, but the density became larger. When the lignin concentration is too high, it was too hard to form the LRF aerogel.

W. Lee *et al.* [32] studied on preparing resorcinol-tannin-formaldehyde copolymer resins (RTF) by using the bark extract of Taiwan acacia and China fir to substitute part of the resorcinol. From the result, the bark extracts used were extracted from Taiwan acacia and China fir bark with 1% NaOH solution and the content of reactive phenolic materials in Taiwan acacia and China fir bark extracts were 51.6% and 46.5%, respectively. The conventional synthesis condition used for RF resin was certainly not suitable for the RTF copolymer resin. It should be formed the RF prepolymer by reacting the resorcinol with formaldehyde at the first stage, and then the bark extracts added and underwent the copolymerization reaction under acidic condition at the second-stage. The RTF copolymer resins prepared has cold-setting capability. They had higher viscosity, shorter gel time as compared with the RF resin. The RTF copolymer resins could be carried out the gluing application immediately after the hardener was added and had bonding strength the same as RF resin. But the RTF copolymer resins had worse stability and shorter shelf life than RF resin.

A. Szczurek *et al.* [33] studied on the preparation of tannin-formaldehyde carbon aerogels based on organic gels obtained by sol-gel polymerization of tannin with formaldehyde that have been dried with supercritical acetone and pyrolysed at 900 °C. Tannin drastically reduce the cost of the gels and polymerise in a wide range of pHs (3-8), leading to porous carbonaceous materials whose mesopore fraction ranges from 57% to 78%. The surface area and the total porosity can be as high as 715 m<sup>2</sup> g<sup>-1</sup> and 95%, respectively. Pore volume and micro-mesopore-size distributions are similar to those of much more expensive carbon aerogels derived from resorcinol-formaldehyde resin. However, more easily adjustable pore textures may be obtained using tannins as precursors.

G. Amarat-Labat *et al.* [34] studied on the preparation of organic carbon cryogel by sol-gel polycondensation of resorcinol (R) and formaldehyde (F) in the presence of mimosa tannin (T). The study showed that 2/3 in weight of the resorcinol can advantageously be replaced by tannin, and that resultant TRF organic gels can be freeze-dried and pyrolysed. The resultant low-cost carbon gels present similar pore texture than those of their expensive aerogel counterparts prepared from pure RF

resin. However, the presence of tannin allows additional features that are encountered in a much lower extent in RF carbon gels. These materials can indeed be prepared from a much broader range of pHs (2-8), leading to pore-size distributions that are progressively shifted towards narrower pores when the pH increases. At pH 8, the carbons are poorly porous, whereas surface areas close to  $650 \text{ m}^2 \text{ g}^{-1}$  are found at low and moderate pHs.

## CHAPTER III

### EXPERIMENTAL PROCEDURE

All experiments in this research are carried out in laboratory-scale to study for the dissolution and regeneration of lignocellulosic residues from agricultural wastes and the preparation of hierarchical porous carbon monolith. The carbon monolith with various porous characteristics are synthesized by sol-gel polycondensation of resorcinol and formaldehyde mixed with lignin (L), hemicelluloses (H) and lignocellulosic materials (LCM). In addition, the composition of lignocellulosic materials regenerated from betel palm is studied. The influences of lignin (L), hemicelluloses (H) and lignocellulosic materials (LCM) on pore structures, porous properties and chemical structures are investigated.

The chemicals, equipments, characterizations and experimental methods in this research are described in this chapter.

#### 3.1 Chemical reagents

The chemical reagents used in this research are showed in Table 3.1

Table 3.1 List of chemical reagents in this research

| Chemical reagents                                                | Grade            | Manufacturer               |
|------------------------------------------------------------------|------------------|----------------------------|
| 1. Sodium hydroxide (NaOH)                                       | Analytical grade | Unilab, New Zealand        |
| 2. Hydrogen peroxide (H <sub>2</sub> O <sub>2</sub> )            | Analytical grade | Unilab, New Zealand        |
| 3. Sulfuric acid (H <sub>2</sub> SO <sub>4</sub> )               | Analytical grade | Qrec, New Zealand          |
| 4. Resorsinol (C <sub>6</sub> H <sub>4</sub> (OH) <sub>2</sub> ) | 99.8% BDH/38     | Fluka, Germany             |
| 5. Formaldehyde (HCOH)                                           | Analytical grade | Ajax Finechem, New Zealand |

Table 3.1 (Next) List of chemical reagents in this research

| Chemical reagents                  | Grade            | Manufacturer                                               |
|------------------------------------|------------------|------------------------------------------------------------|
| 6. Nitric acid (HNO <sub>3</sub> ) | Analytical grade | Ajax Finechem, New Zealand                                 |
| 7. Deionized water                 | -                | Production from MilliQ apparatus (Millipore, Bedford, MA). |
| 8. Lignin, alkali                  | Analytical grade | Sigma Aldrich, USA                                         |
| 9. Xylan, from beechwood           | Analytical grade | Sigma Aldrich, USA                                         |
| 10. Nitrogen (N <sub>2</sub> )     | Purity 99.999%   | Thailand Industrial Gas (TIG), Thailand                    |

## 3.2 Equipments

### 3.2.1 Basic equipments

- Digital balance
- Hot plate
- Magnetic bar
- Magnetic stirrer
- Micro pipette
- Freeze dryer
- Hot air oven
- pH meter
- Water bath

### 3.2.2 Horizontal furnace

Carbonization process in this research is carried out with horizontal furnace reactor as shown in Figure 3.1. The furnace is constructed with the main parts showing with the numbers in the Figure 3.1 as followed;



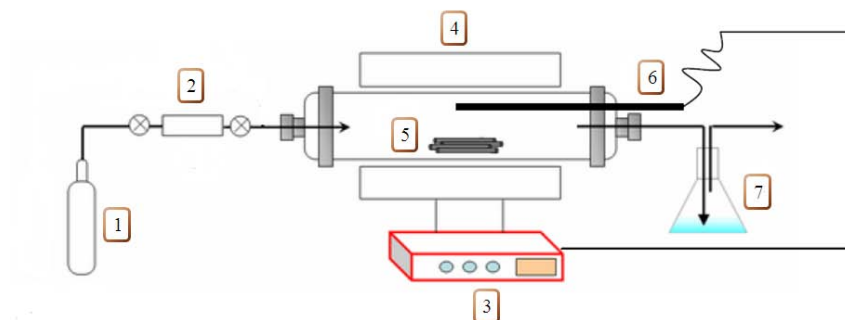


Figure 3.1: Schematic diagram of the quartz tube furnace used in this work, it is composed of (1) N<sub>2</sub> gas container, (2) N<sub>2</sub> gas flow meter, (3) furnace controller, (4) furnace, (5) cylindrical quartz, (6) thermocouple, (7) flask containing alcohol

- Number (1) is the cylindrical gas container of nitrogen 99.999%.
- Number (2) is the gas flow meter of N<sub>2</sub>.
- Number (3) is the furnace controller box.
- Number (4) is the electrical furnace. It can be heated with the power output up to 2000 w.
- Number (5) is the cylindrical quartz tube in a length and diameter of 60 cm and 10 cm, respectively. It is used for holding the samples while being kept in the electrical furnace.
- Number (6) is the thermocouple K-type (maximum temperature 1200 °C)
- Number (7) is the flask contained with ethanol to trap the residue gas.

### 3.3 Characterizations

1. Compositions of lignocellulosic materials were determined by autohydrolysis or hydrothermal treatment method.

2. Porosity was characterized by nitrogen adsorption-desorption at -196 °C (BEL; BELSORP–mini).

2.1 BEL surface ( $S_{\text{BET}}$ ) was determined by BET equation.

2.2 Micropore volume ( $V_{\text{mic}}$ ) was calculated by t-method.

2.3 Mesopore volume ( $V_{\text{mes}}$ ) was calculated by DH-method

3. Microstructure was characterized by SEM (Scanning Electron Microscope) (JEOL; JSM – 5800LV).

4. Fourier Transform Infrared (FTIR) spectra were recorded using spectrometer (Perkin Elmer, 1615).

### 3.4 Experimental Procedures

The experimental procedures in this research can be divided into two main sections. First, the dissolution and regeneration of lignocellulosic residues from agricultural wastes are studied. Second is the preparation of hierarchical porous carbon monolith synthesized by sol-gel polycondensation of resorcinol and formaldehyde mixed with lignin (L), hemicelluloses (H) and lignocellulosic materials (LCM).

#### 3.4.1 Dissolution and regeneration of lignocellulosic residues

In this section, a mixed solution of NaOH/H<sub>2</sub>O<sub>2</sub> was used as a solvent for dissolution of lignocellulosic residues. Rice straw, kapok, luffa and betel palm fiber were used as raw materials. The dissolution was conducted at high temperature as shown in figure 3.1.

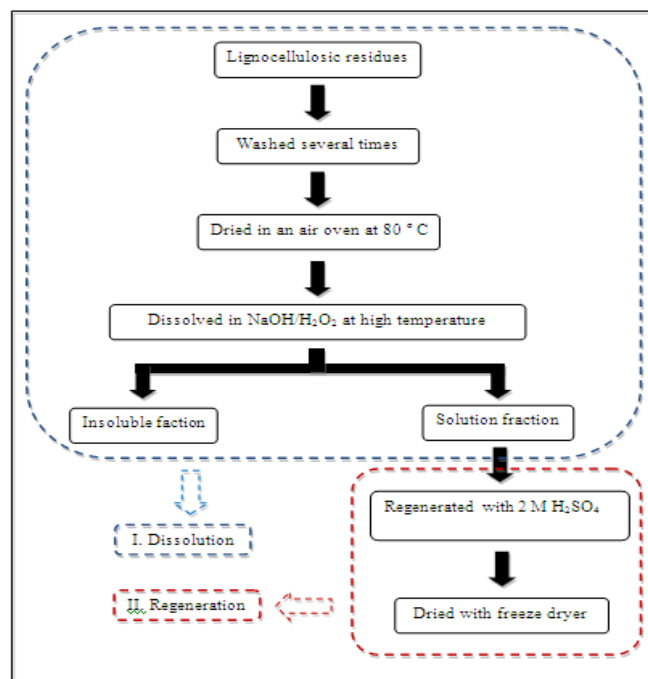


Figure 3.2 Dissolution and regeneration of lignocellulosic residues

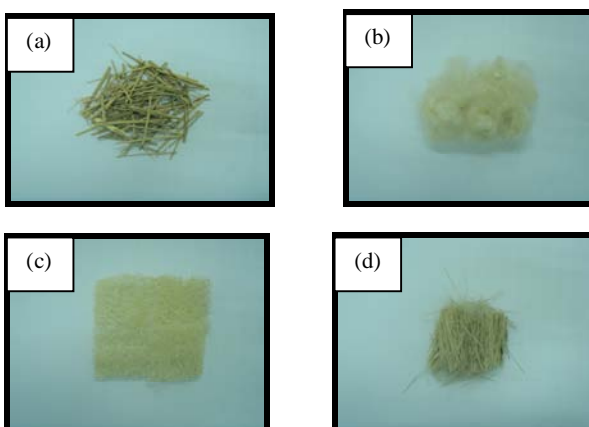


Figure 3.3 Lignocellulosic residues (a) rice straw, (b) kapok, (c) luffa and (d) betel palm fiber

Firstly, lignocellulosic residues were washed several times to ensure good cleaning and dried in an air oven at 80 ° C. Then, the dried fiber was dissolved in a mixed solution of 8% by weight of NaOH and 10% by weight of H<sub>2</sub>O<sub>2</sub> at high temperature during 3 h. After that, the insoluble fraction and the solution fraction were separated. The solution fraction from dissolving the dried fiber in the mixed solution was regenerated with 2 M H<sub>2</sub>SO<sub>4</sub> at room temperature. Finally, a lignocellulosic material (LCM) obtaining from regenerating the solution fraction was washed with distilled water several times until the pH was neutral, and then dried in freeze dryer.

#### 3.4.1.1 Characterization of lignocellulosic materials (LCM)

The composition of lignocellulosic materials was determined by autohydrolysis or hydrothermal treatment method [35].

150 mg of lignocellulosic material was treated with 15 ml of 72% H<sub>2</sub>SO<sub>4</sub> at 30 °C for 3 h. Then, 42 ml of distilled water was added and heated in autoclave at 120 ° C for 1 h. After that, filtration was performed to isolate an insoluble part from clear solution. The pH of the clear solution was adjusted until it became neutral and then the solution was characterized with HPLC and UV-VIS spectroscopy to determine the compositions of hemicellulose and lignin.

### 3.4.2 Preparation of hierarchical porous carbon monolith

The preparation process of hierarchical porous carbon monoliths are shown in figure 3.4.

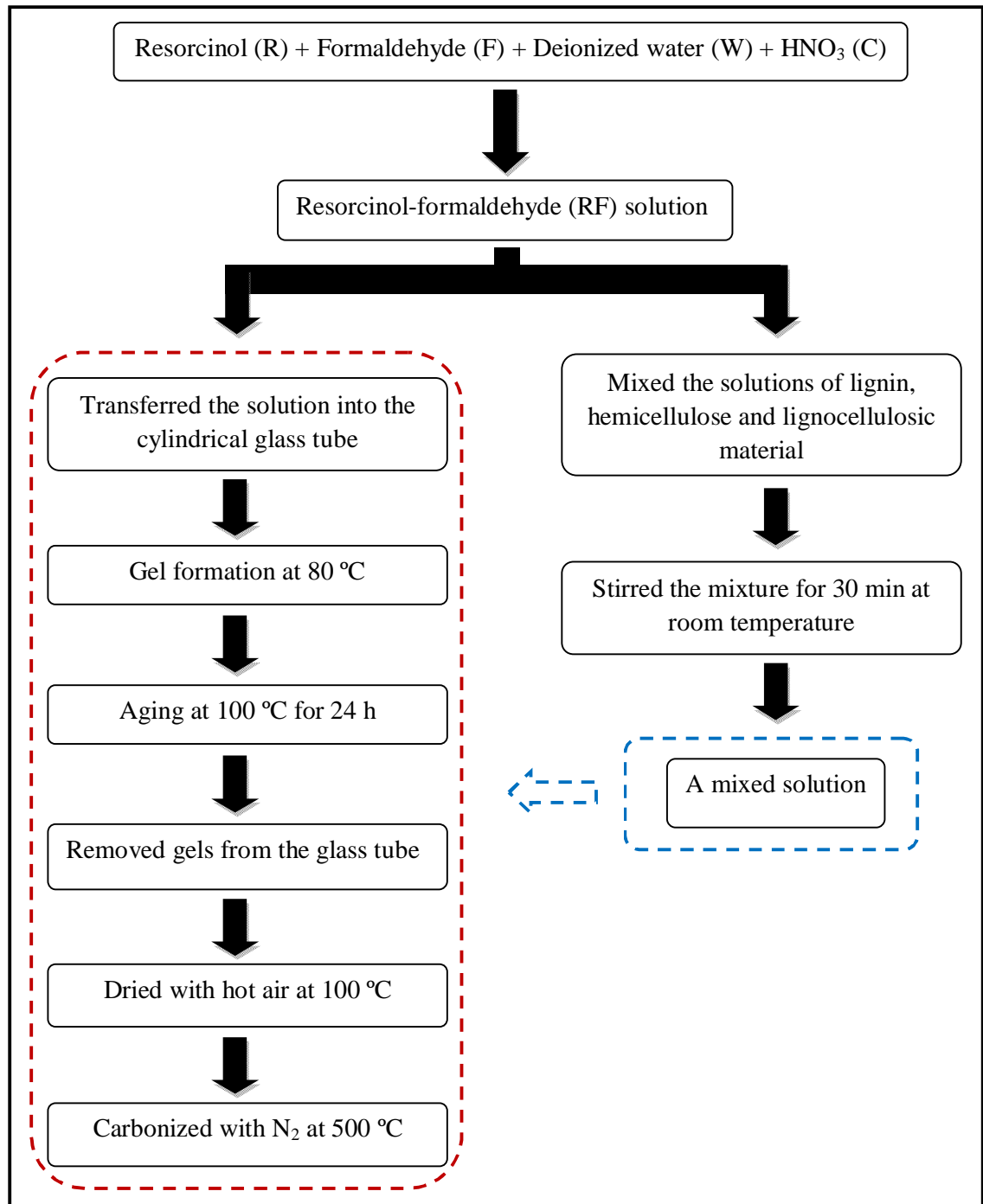


Figure 3.4 Preparation of carbon monolith diagrams

### 3.4.2.1 Preparation of RF gels

Resorcinol-formaldehyde (RF) gels were prepared from resorcinol with formaldehyde in de-ionized water. Nitric acid solution 0.5 M was used as a catalyst.

First of all, resorcinol was dissolved into the deionized water and stirred it with magnetic stirrer until complete solution. Then, the resorcinol solution was added with formaldehyde solution and followed by adding the solution of 0.5 M of nitric acid. The mixture was stirred with magnetic stirrer for 30 min at room temperature. All solutions were then poured in tubes of the inner diameter 1.2 cm which were next sealed and placed in water bath at 80 °C for 24 h, followed by 24 h for aging in the oven at temperature of 100 °C. After aging, the gels were removed from the tube and followed by drying with hot air at 100 °C until the weight was constant. The dried carbon precursors in a monolithic form were obtained.

The molar ratios of resorcinol to formaldehyde (R/F), and resorcinol to water (R/W), and the mole to volume ratio of catalyst to water (C/W) were fixed at 0.5 mol/mol, 0.15 mol/mol and 0.20 mol/ml, respectively.

### 3.4.2.2 Preparation of RF gels mixed lignin (L), hemicellulose (H), lignocellulosic material (LCM)

Lignin (L), hemicellulose (H) and lignicellulosic material (LCM) from betel palm fiber were made into solutions at the concentration 10% by weight before they were used.

At the first stage, the synthesis condition was the same as that for RF gels, and the RF presolution was prepared. The solutions of lignin (L), hemicellulose (H) and lignicellulosic material (LCM) were then added, and the second stage of mixed solution was carried out. Next, the mixture was stirred with magnetic stirrer for 30 min at room temperature. The pH value of the solutions was determined by pH meter. At the second stage, L, H and LCM solutions were added into RF solution at ratio 4:1 and 1:1 volume/volume.

### **3.4.2.3 Carbonization of the RF monolithic gel with N<sub>2</sub>**

The carbon monoliths were prepared by carbonizing the RF monolithic gels in a quartz tube of the horizontal furnace as shown in Figure 3.1. N<sub>2</sub> was used as the carrier gas and flowed through a quartz tube containing the RF monolithic gels at 50 cm<sup>3</sup> (at STP)/min. The furnace was heated at the heating rate of 10 °C/min by starting from room temperature to the temperature of 500 °C. The set point was maintained during 1 h before the furnace was allowed to cool under nitrogen flow. Finally, the carbon monoliths were obtained.

### **3.4.2.4 Characterizations**

The macroporous structures of carbons were revealed by scanning electron microscope (JEOL, JSM-6700F). The micro/meso properties were obtained from the adsorption and desorption isotherms of N<sub>2</sub> at 77 K measured by adsorption apparatus (BEL, mini-BEL Sorp.). Fourier Transform Infrared (FTIR) spectra were recorded using spectrometer (Perkin Elmer 1615).

## CHAPTER IV

### RESULTS AND DISCUSSIONS

The results of the experimental are shown in this chapter. The optimal condition for dissolving lignocellulosic residues and regenerating lignocellulosic solutions, Composition of lignocellulosic materials regenerated from betel palm, Characterizations of the carbon monolith prepared from resorcinol-formaldehyde mixed with lignin (L), hemicelluloses (H), lignocellulosic materials (LCM) and the influence of L, H and LCM on pore structures, porous properties and chemical structures of carbon are explained.

#### 4.1 Dissolution and regeneration of lignocellulosic residues

1 g of lignocellulosic residues (rice straw, kapok, luffa and betel palm fiber) was dissolved in 200 cm<sup>3</sup> of NaOH/H<sub>2</sub>O<sub>2</sub> mixtures (1:1 v/v) at 80 °C until the percentage of solubility was constant.

The dissolution degree, *S*, of lignocellulosic residues is defined by [36]

$$S = \frac{W_o - W_r}{W_o} \times 100 \quad (1)$$

Where *W<sub>r</sub>* is the weight of undissolved lignocellulosic residues, and *W<sub>o</sub>* the original weight of the lignocellulosic residues.

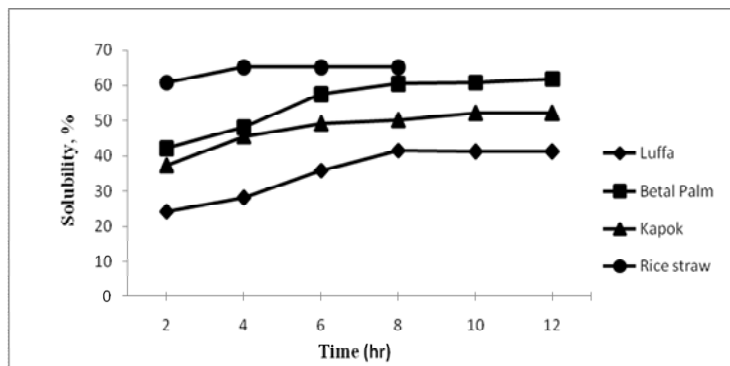


Figure 4.1 Solubility of lignocellulosic residues in NaOH(8wt%)/H<sub>2</sub>O<sub>2</sub>(10wt%) at 80 °C

The optimal condition of a solvent for dissolving lignocellulosic residues is at NaOH (8wt%)/H<sub>2</sub>O<sub>2</sub>(10wt%) and the regeneration of the lignocellulosic solutions was performed at room temperature by using 2 M H<sub>2</sub>SO<sub>4</sub> as a coagulant agent. The ratios between coagulants and solutions were conducted at 1:1 (v/v). Under this condition, betel palm fiber gave the largest amount of regenerated lignocellulosic material (LCM).

#### 4.2 Composition of lignocellulosic materials regenerated from betel palm

Lignocellulosic solution obtaining from dissolving betel palm in NaOH(8wt%)/H<sub>2</sub>O<sub>2</sub>(10wt%) was regenerated by 2 M H<sub>2</sub>SO<sub>4</sub>. Autohydrolysis or hydrothermal treatment method was used to determine the compositions of lignocellulosic materials.

Table 4.1: The compositional data of lignocellulosic materials

| Composition | Weight % |
|-------------|----------|
| Lignin      | 34.51    |
| Xylose      | 64.72    |
| Galactose   | 0.24     |
| Arabinose   | 0.11     |
| Mannose     | 0.32     |

Hemicellulose is made up of amorphous heteropolysaccharides containing different structural units (including xylose, galactose, arabinose and mannose) [35], which can be substituted with phenolic, uronic or acetyl groups. Xylan, made up of the main backbone of xylose units, is the main hemicelluloses component in this material. According to Table 4.1, the lignin and hemicellulose fractions of LCM account for 34.51% and 65.39%, respectively.

#### 4.3 Characterizations of carbon monoliths

Resorcinol (R)-formaldehyde (F) gels mixed with lignin (L), hemicellulose (H), lignocellulosic material (LCM) from betel palm were conducted by carbonization with N<sub>2</sub> to obtain carbon monoliths.



Table 4.2: Synthesis conditions of carbon monolith gels

| Sample name             | Synthesis conditions |       |        |         |      |
|-------------------------|----------------------|-------|--------|---------|------|
|                         | RF/L*                | RF/H* | RF/LH* | RF/LCM* | pH   |
| C                       | -                    | -     | -      | -       | 1.55 |
| C-L                     | 1:1                  | -     | -      | -       | 6.96 |
|                         | 4:1                  | -     | -      | -       | 5.52 |
| C-H                     | -                    | 1:1   | -      | -       | 3.86 |
|                         | -                    | 4:1   | -      | -       | 2.68 |
| C-LH                    | -                    | -     | 1:1    | -       | 5.12 |
|                         | -                    | -     | 4:1    | -       | 3.56 |
| C-LCM (from betel palm) | -                    | -     | -      | 1:1     | 1.97 |
|                         | -                    | -     | -      | 4:1     | 1.85 |

Remark: \* Volume/Volume

At first, the initial pH value of L, H, LH and LCM solutions are at 8.90, 4.33, 6.78 and 3.02 respectively. According to Table 4.2, the pH of mixing solutions can be directly changed by adding L, H, LH and LCM into RF solution as shown in Table 4.2. The parameter pH, therefore, is discussed here for investigation of the final pore structure of the carbon monoliths.

#### 4.3.1 The influence of lignin (L) on porous properties and chemical structure of carbon monolith

The effect of the pH on porous structures on carbon monoliths is studied by SEM, and the micrographs of the interconnected porous texture of the carbon monoliths, C, C-L (4:1) and C-L (1:1) are shown in figure 4.2 (a), (b) and (c), respectively.

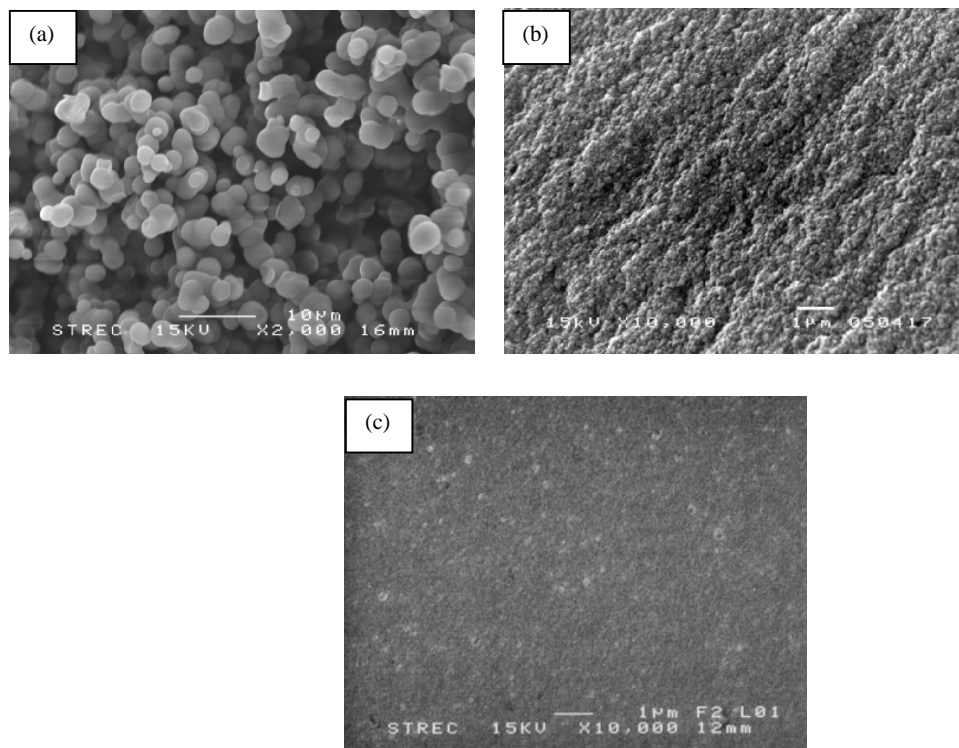


Figure 4.2: SEM images of porous structure of carbon monolith (a) C (RF), (b) C-L (4:1) and (c) C-L (1:1)

Firstly, the initial pH of RF solution for formation of the interconnected macroporous structure is investigated. Figure 4.2 (a) shows that the structure of carbon monolith derived from RF gel prepared at low pH (1.55) is based on a packing of spherical particles. Moreover, when lignin was added into RF solution at ratio 4:1 and 1:1, the pH of the mixture was at 5.52 and 6.96 respectively. From the figure 4.2 (b), the interconnected macropore size of carbon monoliths decrease with increasing initial pH leading to denser structures and even to non-porous carbon for C-L (1:1), see Figure 4.2 (c).

The SEM images clearly indicate that an increase in the initial pH can result in size reduction of the interconnected macropores. The particle size of C is around 2.5 μm which each of the particles appears to be globular and connecting with the others. On the contrary, C-L (4:1) exhibit the interconnected macroporous structure tends to decrease and denser with an increase in initial pH and C-L (1:1) shows that the interconnected macroporous structure cannot be formed in the carbon monolith

prepared from higher than initial pH of 6.9 [4,6]. It can be concluded that the interconnected macroporous texture depends on the initial pH.

The influence of lignin on porous properties on carbon monolith is investigated by nitrogen adsorption-desorption isotherm at 77 K, the BET specific surface area ( $S_{\text{BET}}$ ) and the total pore volume. The  $\text{N}_2$  adsorption-desorption isotherms of sample C, C-L (4:1) and C-L (1:1) are shown in figure 4.3, 4.4 and 4.5 respectively and also the porous properties of the samples are presented in Table 4.3.

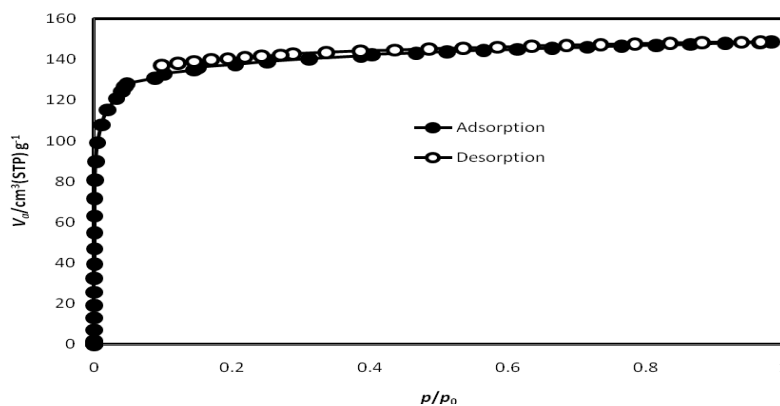


Figure 4.3  $\text{N}_2$  adsorption–desorption isotherm of C-RF

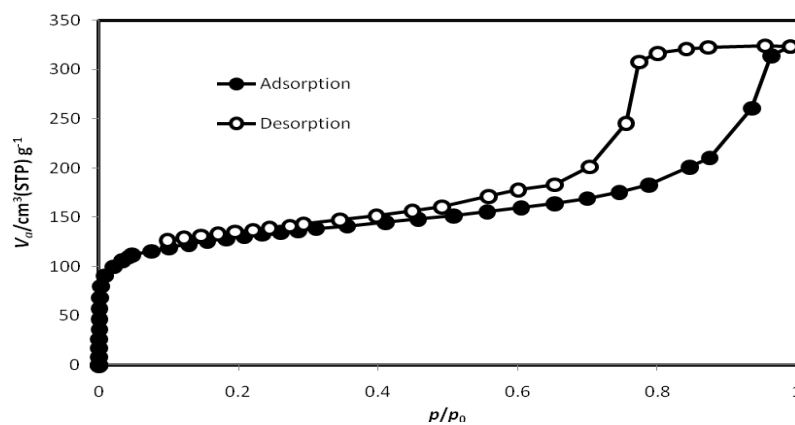


Figure 4.4  $\text{N}_2$  adsorption–desorption isotherm of C-L (4:1)

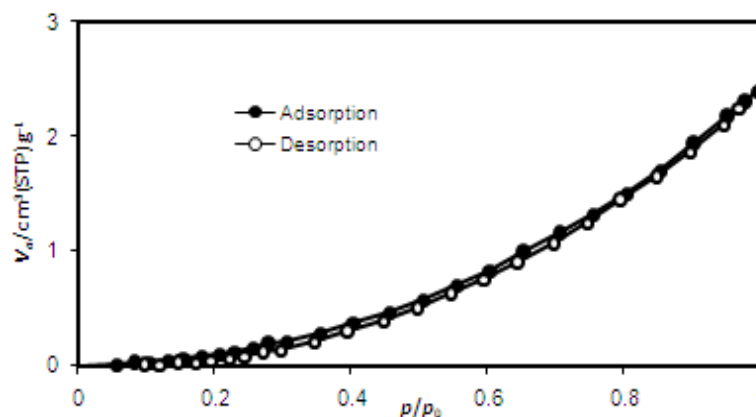
Figure 4.5 N<sub>2</sub> adsorption–desorption isotherm of C-L (1:1)

Table 4.3 Porosity of C-RF and C-L

| Samples   | Pore diameter (nm) | Type of N <sub>2</sub> adsorption-desorption isotherm | Total pore volume (cm <sup>3</sup> /g) | S <sub>BET</sub> (m <sup>2</sup> /g) |
|-----------|--------------------|-------------------------------------------------------|----------------------------------------|--------------------------------------|
| C-RF      | 0.60               | Type I                                                | 0.23±0.01                              | 333±14                               |
| C-L (4:1) | 8.10               | Type IV                                               | 0.98±0.04                              | 482±21                               |
| C-L (1:1) | -                  | Type III                                              | 0.01±0.001                             | 2±0.2                                |

Remark: n=3

From Figure 4.3, nitrogen absorption-desorption isotherm for C-RF is of type I, according to the IUPAC classification, typical of materials includes micropores. In addition, nitrogen absorption-desorption isotherm for C-L (4:1), shown in figure 4.4 is all of type IV, which means that the materials are essentially mesoporous. The BET surface areas (S<sub>BET</sub>) and total pore volume of carbon monoliths derived from RF gel and mixing lignin with RF gel are presented in Table 4.3

According to Table 4.3, the S<sub>BET</sub> of C-RF and C-L (4:1) is 333 and 482 m<sup>2</sup>/g respectively. It is indicated that when lignin was added into RF solution at ratio 4/1 in order to prepare C-L (4:1), the S<sub>BET</sub> of C-L (4:1) is higher than C-RF.

Phenolic molecules are known to react promptly with formaldehyde in both acidic and basic media. At intermediate pH, around 4-5, the cross-linking process is much slower. Slow cross-linking is related to high porosity and high surface areas [32]. For C-RF, during condensation reaction, the colloidal particles of RF can be close to reaction with each other, leading to occurring micropores on the structure of RF. Whereas, For C-L (4:1), when lignin was mixed with RF to prepare the gel, mesopores on the gel structure were obtained instead of micropores. As is well known, lignin is a polymer that has a complex chemical compound, the molecular structure of which contains a large number of phenol units. So, lignin can react with RF molecules and the complex structure of lignin causes the colloidal particles of RF to modify the way to form gels, leading to increasing pore diameter. Consequently, the pore structure of C-L (4:1) is mesoporous. In this context, it is thus not surprising that the highest porosities and BET surface areas correspond to C-L (4:1) prepared at pH 5.52. Nevertheless, for C-L (1:1), carbon monolith was prepared from mixing gel solution at higher pH (6.69). It is interesting to note that C-L (1:1) prepared at high pH is non-porous, see Figure 4.2 (c).

From Table 4.3, It is clearly concluded that lignin can be result in increasing the BET surface areas ( $S_{\text{BET}}$ ) and total pore volume of carbon monoliths. It seems that amounts of lignin in the formulation contributed to significantly broaden the range of pH, leading to increasing the BET surface areas ( $S_{\text{BET}}$ ) for C-L (4:1) and to non-porous for C-L (1:1). Moreover, lignin has an effect on changing  $\text{N}_2$  adsorption-desorption isotherm of carbon monolith from type I into type IV. Thus, mesoporous carbon monolith can be prepared by adding lignin into RF at ratio 4:1.

The chemical structure of C (RF), C-L (4:1) and C-L (1:1) was also analyzed by using FT-IR spectrometer (Perkin Elmer, 1615). In addition, functional groups of lignin and hemicelluloses carbonized at 500 °C are also investigated. Functional groups on surface of carbon can be found in several forms. These functionalities are described in Table 4.4 where the significant peaks from prior study are briefly presented and the typical functional groups and the IR signal of the possible lignin and hemicelluloses are listed in Table 4.5.

Table 4.4: Infrared spectrum peaks for an interpretation of surface functional groups [6].

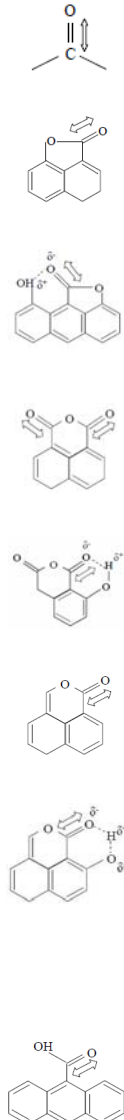
| IR peak bands [cm <sup>-1</sup> ] | Implications                                                                                                                                                                                                                                                                                                                                                                                                                                                                                                                                                  | Chemical form                                                                        |
|-----------------------------------|---------------------------------------------------------------------------------------------------------------------------------------------------------------------------------------------------------------------------------------------------------------------------------------------------------------------------------------------------------------------------------------------------------------------------------------------------------------------------------------------------------------------------------------------------------------|--------------------------------------------------------------------------------------|
| ~ 3200 - 3600                     | Corresponding to functional groups involved in H-bonding (N-H, O- H)<br><br>~ 3400 cm <sup>-1</sup> : corresponding with hydroxyl groups (-OH)<br><br>~ 3600 cm <sup>-1</sup> : corresponding with amine groups (-NH)                                                                                                                                                                                                                                                                                                                                         |                                                                                      |
| ~ 1650 - 1850                     | Corresponding to the functional groups consisting of the bonding C=O vibrations<br><br>~ 1830 cm <sup>-1</sup> : five-membered ring lactone<br><br>~1737 cm <sup>-1</sup> : five-membered ring lactone induced by hydroxyl groups<br><br>~ 1810 -1740 cm <sup>-1</sup> : aldehyde<br><br>~ 1770 – 1670 cm <sup>-1</sup> : aldehyde induced by hydroxyl groups<br><br>~1790 cm <sup>-1</sup> : six-membered ring lactone<br><br>~ 1711 cm <sup>-1</sup> : six-membered ring lactone induced by hydroxyl groups<br><br>~ 1750 cm <sup>-1</sup> : carboxyl group |  |

Table 4.4 (next): Infrared spectrum peaks for an interpretation of surface functional groups.

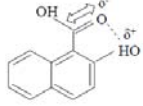
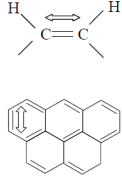
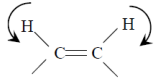
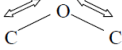
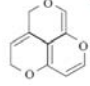
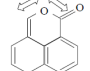
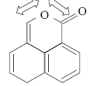
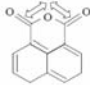
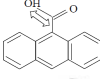
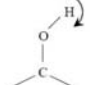
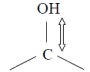
| IR peak bands [cm <sup>-1</sup> ]                          | Implications                                                                                      | Chemical form                                                                         |
|------------------------------------------------------------|---------------------------------------------------------------------------------------------------|---------------------------------------------------------------------------------------|
| ~ 1650 – 1850                                              | ~ 1660 – 1700 cm <sup>-1</sup> : carboxyl group induced by hydroxyl groups                        |    |
| ~ 1550 - 1650                                              | Corresponding with C=C stretching vibration modes of the basal plane of activated carbons         |    |
| ~1350 - 1550                                               | Corresponding to C-H bending vibration mode in basal plane                                        |    |
| ~ 1000 – 1300                                              | Corresponding to C-O stretching vibration modes                                                   |    |
|                                                            | ~ 1025 – 1141 cm <sup>-1</sup> : cyclic ether group                                               |   |
|                                                            | ~1230 – 1250 cm <sup>-1</sup> : ether bridge between rings                                        |  |
|                                                            | ~ 1160 – 1370 cm <sup>-1</sup> : C-O in lactone                                                   |  |
|                                                            | ~ 980 – 1300 cm <sup>-1</sup> : C-O in aldehyde                                                   |  |
|                                                            | ~ 1120 – 1200 cm <sup>-1</sup> : C-O in carboxyl                                                  |  |
| ~ 1000 – 1220 cm <sup>-1</sup> : C-OH stretching vibration | ~ 1160 – 1200 cm <sup>-1</sup> : C-O-H bending vibration                                          |  |
|                                                            | ~ 1000 – 1220 cm <sup>-1</sup> : C-OH stretching vibration                                        |  |
| < 900                                                      | Corresponding to out-of-plane bending vibration of C-C in the basal plane of the activated carbon |                                                                                       |

Table 4.5: The main functional groups of lignin and hemicelluloses [37].

| Wave number (cm <sup>-1</sup> ) | Functional groups                  | Compounds                  |
|---------------------------------|------------------------------------|----------------------------|
| ~3600-3000                      | OH stretching                      | Acid, methanol             |
| ~2860-2970                      | C-H <sub>n</sub> stretching        | Alkyl, aliphatic, Aromatic |
| ~1700-1730, }<br>~1510-1560 }   | C=O stretching                     | Ketone and carbonyl        |
| ~1632                           | C=C                                | Benzene stretching ring    |
| ~1613, 1450                     | C=C stretching                     | Aromatic skeletal mode     |
| ~1470-1430                      | O-CH <sub>3</sub>                  | Methyl-O-CH <sub>3</sub>   |
| ~1440-1400                      | OH bending                         | Acid                       |
| ~1402                           | CH bending                         |                            |
| ~1232                           | C-O-C stretching                   | Aryl-alkyl ether linkage   |
| ~1215                           | C-O stretching                     | Phenol                     |
| ~1170, 1082                     | C-O-C stretching vibration         | Pyranose ring skeletal     |
| ~1108                           | OH association                     | C-OH                       |
| ~1060                           | C-O stretching and C-O deformation | C-OH (ethanol)             |
| ~700-900                        | C-H                                | Aromatic hydrogen          |
| ~700-400                        | C-C stretching                     |                            |

The infrared spectra of carbon monoliths prepared from RF gels (C) and RF/lignin gels (C-L 1:1 and C-L 4:1) are shown in Figure 4.6 (a), (b) and (c), respectively. These carbons are obtained by carbonization with N<sub>2</sub>. In addition, Figure 4.6 (d) shows the infrared spectra of lignin carbonized at 500 °C.



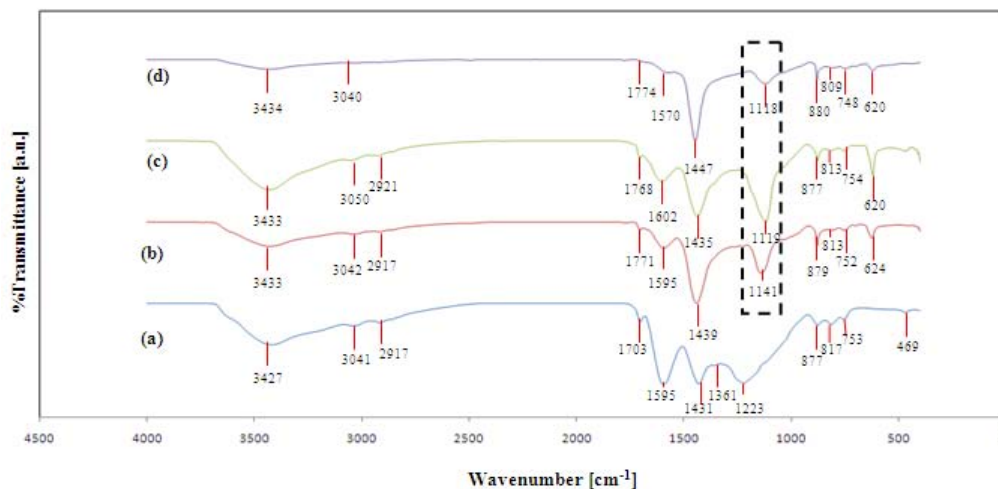


Figure 4.6 FTIR spectra of the (a) C (RF), (b) C-L (1:1), (c) C-L (4:1) and (d) lignin carbonized at 500 °C

According to the Figure 4.6 (a), the infrared spectra of functional groups on surface of carbon monolith prepared from RF gel (C) is discussed. The peak at 3427  $\text{cm}^{-1}$  is assigned to hydroxyl or phenol groups. The peak in range of 2800-3200  $\text{cm}^{-1}$ , in this work at 3041 and 2917  $\text{cm}^{-1}$  are attributed to C-H stretching and  $-\text{CH}_2$  stretching in methylene bridge, respectively. The peak band at around 1703 and 1595  $\text{cm}^{-1}$  can be ascribed to the aromatic skeleton stretching and C=C stretching vibration modes. The peak at 1431 and 1361  $\text{cm}^{-1}$  can be assigned to phenolic-OH in plane deformation. The peak at 1223  $\text{cm}^{-1}$  can be ascribed to C-O-C linkage stretching between two resorcinol molecules. The peak band below 900  $\text{cm}^{-1}$  may be attributed to C-C out-of-plane bending at substituted positions in aromatic ring.

According to Figure 4.6 (d), the infrared spectra of lignin carbonized at 500 °C is shown. The peaks are somewhat similar to C (RF) at around 3434, 3040, 1774 and 1570  $\text{cm}^{-1}$ . However, there is a peak at 1118  $\text{cm}^{-1}$  attributed to C-O-C stretching vibration of lignin molecules.

From the Figure 4.6 (b) and (c), the infrared spectra of C-L (1:1) and C-L (4:1) are considered. The curves are nearly identical with C (RF), except a few that can be explained as follows. The much sharper peaks at around 1110  $\text{cm}^{-1}$  of C-L (1:1) and C-L (4:1) as compared with lignin carbonized at 500 °C and the absence of the peaks

at  $1223\text{ cm}^{-1}$  in C-L (1:1) and C-L (4:1) indicate that cross-linking by reaction between lignin and resorcinol-formaldehyde has indeed occurred.

In summary, the chemical structures of carbon monolith prepared from RF/lignin gels (C-L 1:1 and C-L 4:1) are different from C (RF) in certain parts, as there is a cross-linking of between lignin and resorcinol-formaldehyde molecules on carbon monolith prepared from RF/lignin gels (C-L 1:1 and C-L 4:1). That leads to changing the chemical structure of C-L (1:1) and C-L (4:1).

#### 4.3.2 The influence of hemicellulose (H) on porous properties and chemical structure of carbon monolith

The effect of the hemicelluloses (from beechwood, Sigma Aldrich) on porous structures on carbon monoliths is studied by SEM, and the micrographs of the interconnected porous texture of the carbon monoliths, C-H (4:1) and C-H (1:1) are shown in figure 4.7 (a) and (b) respectively.

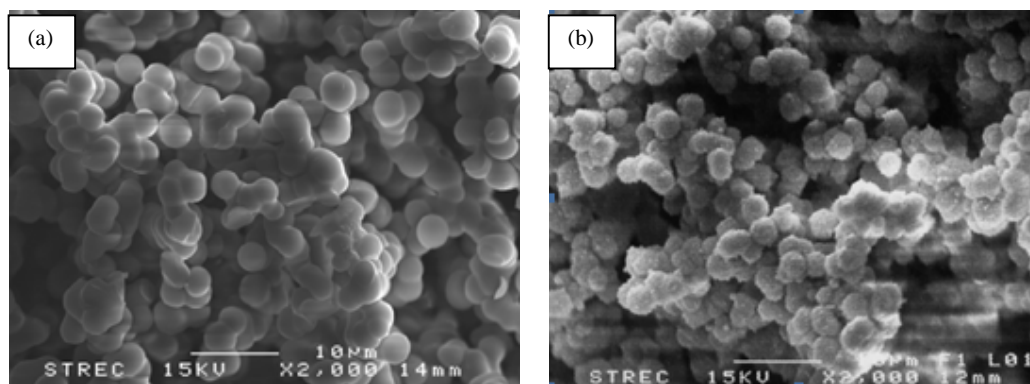


Figure 4.7: SEM images of porous structure of carbon monolith (a) C-H (4:1) and (b) C-H (1:1)

Figure 4.7 (a) and 4.7 (b) show that the structure of carbon monolith is based on a packing of spherical particles similar to C (RF), see Figure 4.2 (a). The SEM images indicate that the presence of hemicelluloses in the formulation does not lead to changing the structure of carbon monolith. These structures result from the initial pH of gels of C-H (4:1) and C-H (1:1) which is at 2.68 and 3.86, respectively. The nodules has diameters strongly depending on the initial pH of gel solutions, ranging

from more than 100 to less than 50 nm at low and high pH, respectively [32]. As seen in Figure 4.7 (a) and 4.7 (b), the nodules of C-H (4:1) and C-H (1:1) have a diameter ranging from 200-250 nm.

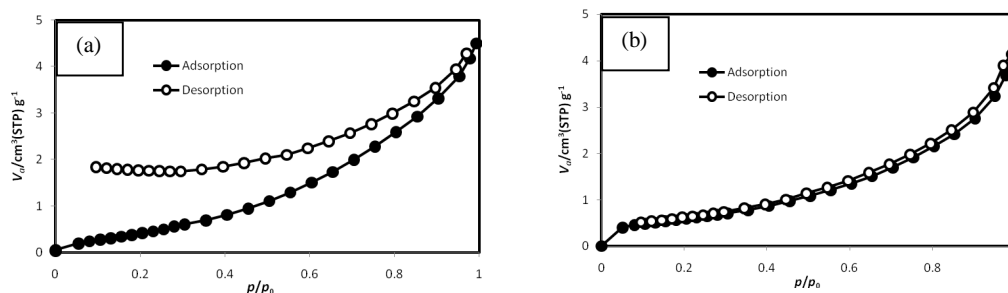


Figure 4.8  $N_2$  adsorption–desorption isotherm of (a) C-H (4:1) and (b) C-H (1:1)

Table 4.6 Porosity of C-H

| Samples   | Pore diameter<br>(nm) | Type of $N_2$<br>adsorption-<br>desorption isotherm | Total pore<br>volume<br>( $cm^3/g$ ) | $S_{BET}$ ( $m^2/g$ ) |
|-----------|-----------------------|-----------------------------------------------------|--------------------------------------|-----------------------|
| C-H (4:1) | ND                    | *                                                   | $0.01 \pm 0.001$                     | $3 \pm 0.3$           |
| C-H (1:1) | ND                    | *                                                   | $0.01 \pm 0.001$                     | $27 \pm 5$            |

Remark: ND = not determined, \* = unidentified type, n = 3

The influence of hemicellulose on porous properties on carbon monolith is investigated by nitrogen adsorption-desorption isotherm at 77 K, From Figure 4.8 (a) and 4.8 (b), nitrogen adsorption-desorption isotherm for C-H (4:1) and C-H (1:1) are an unidentified type, according to the IUPAC classification.

Moreover, the  $N_2$  adsorption-desorption isotherms of sample C-H (4:1) and C-H (1:1) reveal that micropores on C-RF structure are disappeared when hemicellulose is mixed to prepare carbon monoliths. As there is no phenol unit on the structure of hemicellulose component (xylose, galactose, arabinose and mannose). Thus, hemicellulose cannot react with RF like lignin therefore it has no effect on reaction of RF molecules during gel formation but fills inside microporous structure of gels

instead. Furthermore, when the gels are carbonized at 500 °C, hemicellulose is degraded at this temperature and RF gels are certainly shrunk, leading to closing micropores on carbon monolith structure. Therefore, the microporous structure is disappeared. So, This can be concluded that hemicellulose has an impact on microporous structure of obtained carbon monoliths.

Moreover, the infrared spectra of carbon monoliths prepared from RF gels (C) and RF/hemicellulose gels (C-H 1:1 and C-H 4:1) are shown in Figure 4.9 (a), (b) and (c), respectively. These carbons are obtained by carbonization with N<sub>2</sub>. In addition, Figure 4.9 (d) shows the infrared spectra of hemicelluloses carbonized at 500 °C.

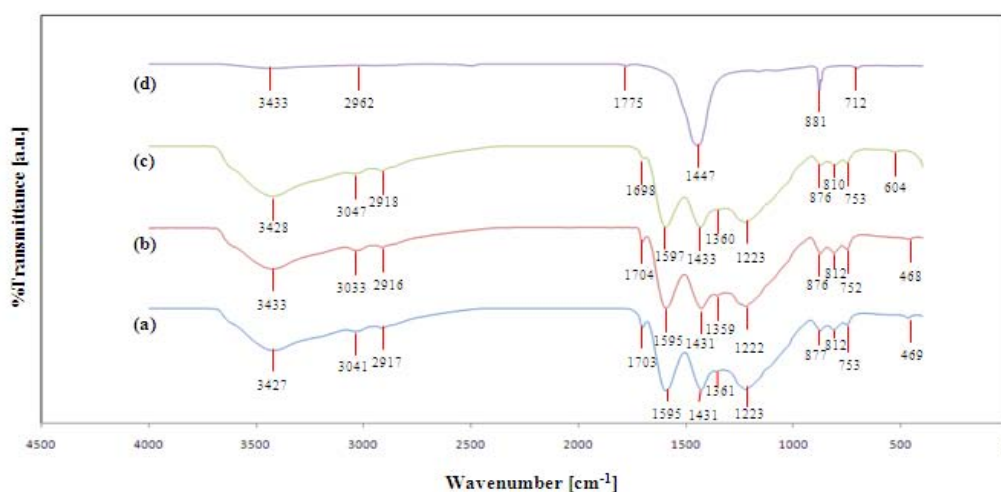


Figure 4.9 FTIR spectra of the (a) C (RF), (b) C-H (1:1), (c) C-H (4:1) and (d) hemicellulose carbonized at 500 °C

According to Figure 4.9 (a), (b) and (c), the FTIR spectra of C (RF), C-H (1:1) and C-H (4:1) reveals that the spectra are similar. The interesting peaks are at around 3433, 3033, 2916, 1704, 1595, 1430-1360 and 1222 cm<sup>-1</sup> attributed to hydroxyl or phenol groups, C-H stretching, -CH<sub>2</sub> stretching in methylene bridge, aromatic skeleton stretching, C=C stretching vibration modes, phenolic-OH in plane deformation and C-O-C linkage stretching between two resorcinol molecules, respectively.

From figure 4.9 (d), the infrared spectra of hemicelluloses carbonized at 500 °C is considered. There is a remarkable peak appearing at around 1430-1360 cm<sup>-1</sup>

similar to C (RF), C-H (4:1) and C-H (1:1). The peak is at  $1466\text{ cm}^{-1}$  ascribed to methoxyl-O-CH<sub>3</sub> of hemicelluloses structure.

In conclusion, because of the similar infrared spectra curves of C (RF), C-H (1:1) and C-H (4:1), this suggests that hemicelluloses in C-H (1:1) and C-H (4:1) cannot react with RF. Moreover, when the gels are carbonized at  $500\text{ }^{\circ}\text{C}$ , hemicellulose is degraded at this temperature. Hence, carbon monoliths prepared from RF gels (C) and RF/hemicellulose gels (C-H 1:1 and C-H 4:1) have a similar chemical structure.

### 4.3.3 The influence of lignocellulosic materials (LCM) on porous properties and chemical structure of carbon monolith

In this section, the influence of the lignocelulosic materials from betel palm on porous structures on carbon monoliths is studied by SEM, and the micrographs of the interconnected porous texture of the carbon monoliths, C-LCM (4:1), C-LCM (1:1), C-LH (4:1) and C-LH (1:1) are shown in figure 4.10 (a), (b), (c) and (d) respectively. Furthermore, porous properties and chemical structure between C-LCM and C-LH are compared.

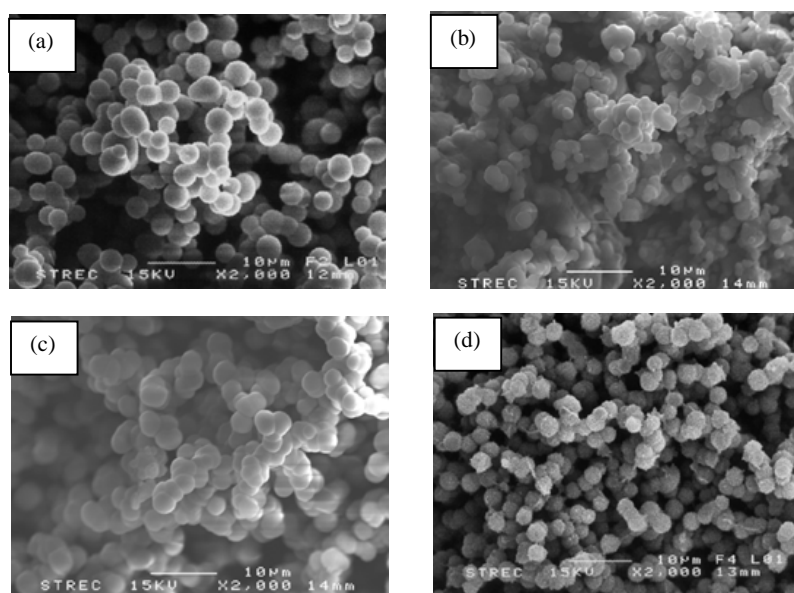


Figure 4.10: SEM images of porous structure of carbon monolith (a) C-LCM (4:1), (b) C-LCM (1:1), (c) C-LH (4:1) and (d) C-LH (1:1)

Figure 4.10 (a), (b), (c) and (d) shows that the structure of carbon monolith is based on a packing of spherical particles very similar to C-H (4:1) and C-H (1:1) see Figure 4.7 (a) and (b). This result indicates that hemicellulose has a more influence on pore structure than lignin because it is the main component (65%) of LCM and LH. In addition, because of the initial pH of gel solutions at around 2-5, Figure 4.10 (a)-4.10 (d) reveal that the nodules of C-LCM (4:1), C-LCM (1:1), C-LH (4:1) and C-LH(1:1) have a diameter ranging from 125-250 nm. This can be explained in the same reason for C-H (4:1) and C-H (1:1)

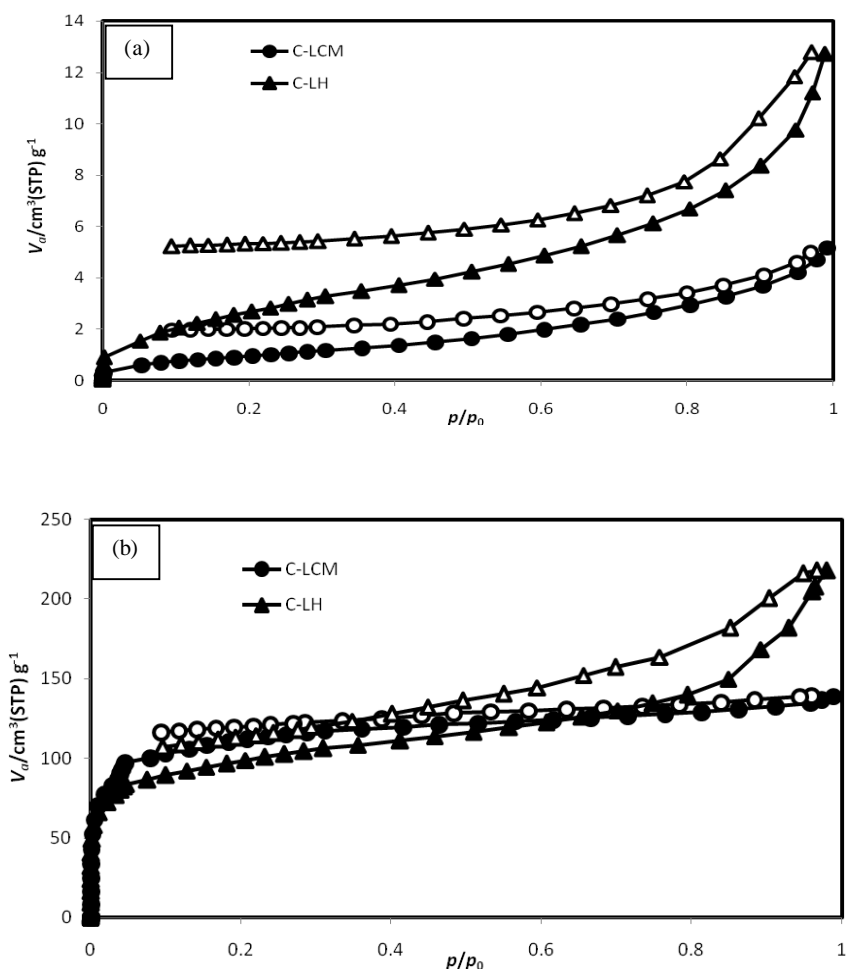


Figure 4.11  $\text{N}_2$  adsorption-desorption isotherm of (a) C-LCM, C-LH (4:1) and (b) C-LCM, C-LH (1:1)

Table 4.7 Porosity of C-LCM and C-LH

| Samples     | Pore diameter (nm) | Type of N <sub>2</sub> adsorption-desorption isotherm | Total pore volume (cm <sup>3</sup> /g) | S <sub>BET</sub> (m <sup>2</sup> /g) |
|-------------|--------------------|-------------------------------------------------------|----------------------------------------|--------------------------------------|
| C-LCM (4:1) | ND                 | *                                                     | 0.03±0.003                             | 24±4                                 |
| C-LCM (1:1) | ND                 | *                                                     | 0.13±0.01                              | 134±20                               |
| C-LH (4:1)  | ND                 | *                                                     | 0.01±0.001                             | 10±3                                 |
| C-LH (1:1)  | ND                 | *                                                     | 0.34±0.01                              | 270±15                               |

Remark: ND = not determined, \* = unidentified type, n = 3

The influence of LCM and LH on porous properties on carbon monolith is investigated by nitrogen adsorption-desorption isotherm at 77 K.

From Figure 4.11 (a), nitrogen adsorption-desorption isotherms of both C-LCM and C-LH at the ratio 4:1 look almost similarly. Moreover, from Figure 4.11 (b), at the ratio 1:1 of C-LCM and C-LH are quite identical. All N<sub>2</sub> adsorption-desorption isotherms of C-LCM and C-LH are an unidentified type, according to the IUPAC classification.

From the SEM images and nitrogen adsorption-desorption isotherms of C-LCM and C-LH can be concluded that carbon monoliths prepared from LCM (lignocellulosic materials) and LH (lignin/hemicellulose) mixed with resorcinol-formaldehyde at the same ratio have similar pore structure and porous properties.

According to Table 4.7, the S<sub>BET</sub> of C-LCM (1:1) and C-LH (1:1) is 134 and 270 m<sup>2</sup>/g respectively. It is indicated that the S<sub>BET</sub> of C-LH (1:1) is higher than C-LCM (1:1) and it seems that lignin can react with RF, leading to increasing surface area because of the initial pH of C-LH (1:1) at 5.12, see Table 4.2.

In addition, the infrared spectra of carbon monoliths prepared from RF gels (C) and RF/lignocellulosic material gels (C-LCM 1:1 and C-LCM 4:1) are shown in Figure 4.12 (a), (b) and (c), respectively. These carbons are obtained by carbonization

with N<sub>2</sub>. In addition, Figure 4.12 (d) and (e) shows the infrared spectra of lignin and hemicelluloses carbonized at 500 °C, respectively.

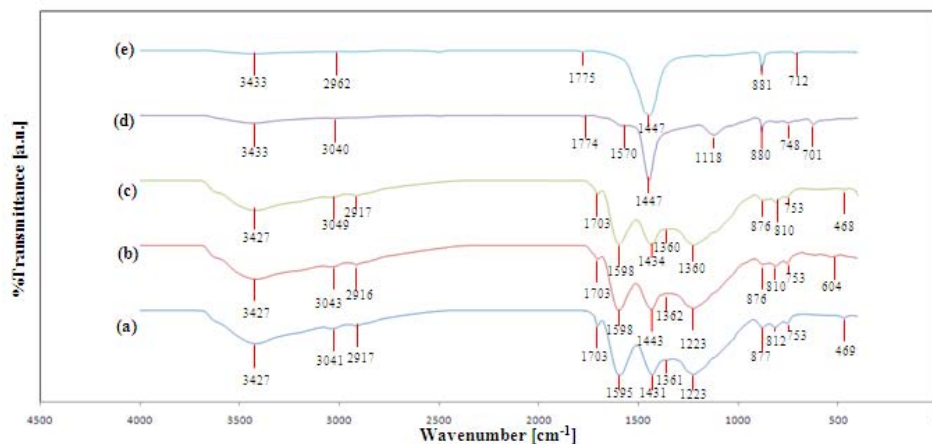


Figure 4.12 FTIR spectra of the (a) C (RF), (b) C-LCM (1:1), (c) C-LCM (4:1), (d) lignin and (e) hemicellulose carbonized at 500 °C

From the Figure 4.12 (a), (b) and (c), the FTIR spectra of C (RF), C-LCM (1:1) and C-LCM (4:1) are discussed. The infrared spectra curves of C (RF) and C-LCM are alike. Moreover, C-LCM (1:1) and C-LCM (4:1) have similar curves with C-H (1:1) and C-H (4:1) as previously mentioned in the section 4.2.2 (Figure 4.9). It seems that a part of lignin in lignocellulosic materials has no reaction with resorcinol-formaldehyde because of their initial pH of RF/lignocellulosic material gels. Furthermore, both lignin and hemicelluloses are degraded from C-LCM (1:1) and C-LCM (4:1) after carbonizing with N<sub>2</sub> at 500 °C.

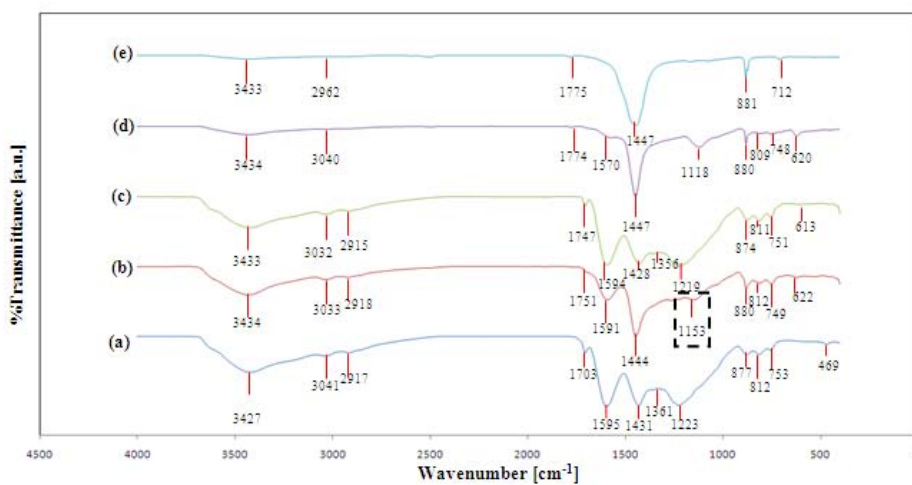


Figure 4.13 FTIR spectra of the (a) C (RF), (b) C-LH (1:1), (c) C-LH (4:1), (d) lignin and (e) hemicellulose carbonized at 500 °C



Moreover, the chemical structure of C-LH (1:1) and C-LH (4:1) are studied. According to 4.13 (a), (b) and (c), the FTIR spectra of C (RF), C-LH (1:1) and C-LH (4:1) are considered. For C-LH (4:1), the infrared spectra curve is similar to C-H (1:1), C-H (4:1), C-LCM (1:1) and C-LCM (4:1). However, in case of C-LH (1:1), there is a peak at  $1153\text{ cm}^{-1}$  attributed to C-O-C stretching vibration of lignin. With the same reason of C-L (1:1) and C-L (4:1) as previously explained in the section 4.2.1, cross-linking by reaction between a part of lignin in LH and resorcinol-formaldehyde has occurred.

In summary, when the chemical structures of C-LCM and C-LH are compared, it is found that C-LCM (4:1) and C-LH (4:1) have a similar structure. However, for C-LCM (1:1) and C-LH (1:1), the infrared spectra curves are different because the reaction of lignin and resorcinol-formaldehyde has occurred in case of C-LH (1:1). On the contrary, for C-LCM (1:1), a part of lignin in lignocellulosic materials has no reaction with resorcinol-formaldehyde. It seems to be that chemical structure of these carbons depends on the initial pH of each sample as shown in Table 4.2 and also lignin seems to react with resorcinol-formaldehyde at pH around 5-7.

## **CHAPTER V**

### **CONCLUSIONS**

First, the optimal condition for dissolution and regeneration of lignocellulosic residues and the composition of lignocellulosic materials regenerated from betel palm were described. Second, the effect of lignin, hemicelluloses and lignocellulosic materials on porous properties and chemical structure were investigated.

#### **5.1 The optimal condition for dissolution and regeneration of lignocellulosic residues**

The optimal condition of the solvent for dissolving lignocellulosic residues (rice straw, kapok, luffa and betel palm) is at NaOH (8wt%)/H<sub>2</sub>O<sub>2</sub>(10wt%) and the regeneration of the lignocellulosic solutions was performed at room temperature by using 2 M H<sub>2</sub>SO<sub>4</sub> as a coagulant agent. The ratios between coagulants and solutions were conducted at 1:1 (v/v). Under this condition, the regeneration of the lignocellulosic solution from betel palm fiber yields the most lignocellulosic material (LCM) and the lignin and hemicelluloses fractions of lignocellulosic materials are 34.51% and 65.39%, respectively.

#### **5.2 The porous properties and chemical structure of carbon monolith**

Firstly, Physical properties of C-L obtained from carbonization are investigated by nitrogen adsorption-desorption isotherm and SEM. The result shows that lignin has a crucial role to change properties of the carbon monoliths. At first, carbon monoliths obtained from resorcinol-formaldehyde gel (C-RF) are found to be microporous carbon. The microporosity, whose BET surface area ( $S_{\text{BET}}$ ) and total pore volume are 333 m<sup>2</sup>/g and 0.23 cm<sup>3</sup>/g, respectively. When lignin is added in to RF solution at pH 5.5 to prepare C-L (4:1), the carbon monolith is essentially mesoporous. Also, lignin can be result in increasing BET surface area ( $S_{\text{BET}}$ ) and total pore volume of the carbon monolith (482 m<sup>2</sup>/g and 0.98 cm<sup>3</sup>/g). Nevertheless, for C-L (1:1), carbon monolith is prepared from mixing gel solution at pH 6.69, the SEM

micrograph reveals that C-L (1:1) is non-porous carbon. From the result of SEM and nitrogen adsorption-desorption isotherm of carbon monolith, it is obviously seen that the initial pH has an influence on properties of carbon monolith. Furthermore, from the result of FT-IR, the chemical structures of carbon monolith prepared from RF/lignin gels (C-L 1:1 and C-L 4:1) are different from C (RF) in certain parts, as there is a cross-linking of between lignin and resorcinol-formaldehyde molecules on carbon monolith prepared from RF/lignin gels (C-L 1:1 and C-L 4:1). That leads to changing the chemical structure of C-L (1:1) and C-L (4:1), For C-L (4:1), at pH 5.5, the cross linking is much slower, slow cross-linking is related to high porosity and high surface area. On the contrary, C-L (1:1) shows that the interconnected macroporous structure cannot be formed in the carbon monolith prepared from higher than initial pH of 6.9.

Secondly, the influence of hemicelluloses on physical properties of C-H (4:1) and C-H (1:1) is investigated. The SEM images show that the structure of carbon monolith is based on a packing of spherical particles similar to C (RF). This result indicates that the presence of hemicelluloses in the formulation does not lead to changing the structure of carbon monolith. In addition, from the adsorption-desorption isotherm results, it can be seen that micropores on C-RF structure are disappeared when hemicellulose is mixed to prepare carbon monoliths. So, This can be concluded that hemicellulose has an impact on microporus structure of obtained carbon monoliths. Because of the similar infrared spectra curves of C (RF), C-H (1:1) and C-H (4:1), this suggests that hemicelluloses in C-H (1:1) and C-H (4:1) cannot react with RF. Moreover, when the gels are carbonized at 500 °C, hemicellulose is degraded at this temperature. Hence, carbon monoliths prepared from RF gels (C) and RF/hemicellulose gels (C-H 1:1 and C-H 4:1) have a similar chemical structure.

Finally, the comparison of porous properties and chemical structure between C-LCM and C-LH is studied. From the SEM images and nitrogen adsorption-desorption isotherms of C-LCM and C-LH can be obviously seen that carbon monoliths prepared from LCM (lignocellulosic materials) and LH (lignin/hemicellulose) mixed with resorcinol-formaldehyde at the same ratio have

similar pore structure. Moreover, when the chemical structures of C-LCM and C-LH are compared, it is found that C-LCM (4:1) and C-LH (4:1) have a similar structure. However, for C-LCM (1:1) and C-LH (1:1), the infrared spectra curves are different because the reaction of lignin and resorcinol-formaldehyde seems to occur in case of C-LH (1:1). On the contrary, for C-LCM (1:1), a part of lignin in lignocellulosic materials has no reaction with resorcinol-formaldehyde. It seems that chemical structure of these carbons depends on the initial pH of each sample and lignin seems to react with resorcinol-formaldehyde at pH around 5-7

## REFERENCES

- [1] Sun, R.C., Fang, J.M., and Tomkinson, J. Delignification of rye straw using hydrogen peroxide. Industrial Crops and Products 12 (2000): 71–83.
- [2] Ghali, L., Msahli, S., Zidi, M., and Sakli, F. Effect of pre-treatment of Luffa fibres on the structural properties. Materials Letters 83 (2009): 61-63.
- [3] Muhammad, N., Man, Z., Bustam, M.A., and Rafiq S. Dissolution and delignification of bamboo biomass using amino acid-based ionic liquid. Appl Biochem Biotechnol 1 (20011): 1-12.
- [4] Lin, C., and Ritter, J.A. Effect of synthesis pH on the structure of carbon xerogels. Carbon 35 (1997): 1271-1278.
- [5] Chajjitrakool, T., Tonanon, N., Tanthapanichakoon, W., Tamon, H., and Prichanont, S. Effects of pore characters of mesoporous resorcinol–formaldehyde carbon gels on enzyme immobilization. Journal of Molecular Catalysis B: Enzymatic 55 (2008): 137–141.
- [6] Adisak Siyasukh. Preparation of hierarchical porous carbon monolith without using templates. Doctoral Dissertation, Department of Chemical Engineering, Faculty of Engineering, Chulalongkorn University, 2008.
- [7] Yamamoto, T., Mukai, S.R., Endo, A., Nakaiwa, M., and Tamon, H. Interpretation of structure formation during the sol-gel transition of a resorcinol-formaldehyde solution by population balance. Journal of Colloid and Interface Science 264 (2003): 532–537.
- [8] Pekala, R.W. Organic aerogels from the polycondensation of resorcinol with formaldehyde. Journal of materials 24 (1989): 3221-3227.
- [9] Pahl, R., Bonser, U., Pekala, R.W., and Kinney, J.H. SAXS Investigations on Organic Aerogels. Journal of Applied Crystallography 24 (1991): 771-776.
- [10] Yamamoto, T., Yoshida, T., Suzuki, T., Mukai, S.R., and Tamon, H. Dynamic and Static Light Scattering Study on the Sol-Gel Transition of Resorcinol-

- Formaldehyde Aqueous Solution. Journal of Colloid and Interface Science 245 (2002): 391–396.
- [11] Yamamoto, T., Nishimura, T., Suzuki, T., and Tamon, H. Effect of drying method on mesoporosity of resorcinol-formaldehyde drygel and carbon gel. Drying Technology 19(7) (2001): 1319–1333.
- [12] Shakeri, M., and Kawakami, K. Effect of the structural chemical composition of mesoporous materials on the adsorption and activation of the *Rhizopus oryzae* lipase-catalyzed trans-esterification reaction in organic solvent. Catalysis Communications 10 (2008): 165–168.
- [13] Chen, F., Xu, M., Wang, L., and Li, J. Preparation and characterization of organic aerogels from a lignin-resorcinol-formaldehyde copolymer. Bioresource 6(2) (2011): 1262-1762.
- [14] Rossouw, D., Du, T., Pizzi, A., and McGillivray, G. The kinetics of condensation of phenolic polyflavonoid tannins with aldehyde. Polym Sci Polym Chem 18 (1980): 3323-3343.
- [15] Stöcker, M. Biofuels and biomass to liquid fields in the biorefinery: Catalytic conversion of lignocellulosic biomass using porous materials. Angew. Chem. Int. Ed. 47 (2008): 9200-9211.
- [16] Derkacheva, O., and Sukhov, D. Investigation of lignins by FTIR spectroscopy. Macromol. Symp. 265 (2008): 61-68.
- [17] Muhammad, N., Man, Z., Khalil, M.A.B., and Elsheikh, Y.A. Dissolution of bamboo (*Gigantochloa scortechinii*) using ionic liquids. Journal of Applied Science (2010): 1-7.
- [18] Kroto, H. W., Heath, J.R., O'Brien, S.C., Curl, R.F., and Smalley, R.E. Nature 318 (1985): 162-263.
- [19] Kowalewski, T., Tsarevsky, N. V., and Matyjaszewski, K. J. Am. Chem. Soc 124 (2002): 10632-10633.
- [20] Tamon, H., and Ishizaka, H. Influence of Gelation Temperature and Catalysts on the Mesoporous Structure of Resorcinol–Formaldehyde Aerogels. Journal of Colloid and Interface Science 223 (2000): 305–307.

- [21] Kato, M., Inuzuka, K., Sakai-Kato, K., and Toyo'oka, T. Monolithic bioreactor immobilization trypsin for high-throughput analysis. Anal Chem 77 (2005): 1813-1818.
- [22] Nakanishi, K., Minakuchi, H., and Soga, N. Double pore silica gel monolith applied to liquid chromatography. J Sol-Gel Sci Techn 8 (1997): 547-552.
- [23] Ikegami, T., and Tanaka, N. Monolithic columns for high-efficiency HPLC separations. Curr Opin Chem Biol 8 (2004): 527-533.
- [24] Fuchigami, T., Toki, M., and Nakanishi, K. Membrane emulsification using sol-gel derived macroporous silica glass. J Sol-Gel Sci Techn 19 (2000): 337-341.
- [25] Chen SX, Zhang X, Shen PK. Macroporous conducting matrix: Fabrication and application as electrocatalyst support. Electrochem Commun 8 (2006): 713-719.
- [26] Zubizarreta, L., Arenillas, A., Pirard, J.P., Pis, J.J., and Job, N. Tailoring the textural properties of activated carbon xerogels by chemical activation with KOH. Microporous and Mesoporous Materials 115 (2008): 480-490.
- [27] Yamamoto, T., Nishimura, T., Suzuki T., and Tamon, H. Effect of drying conditions on mesoporosity of carbon precursors prepared by sol-gel polycondensation and freeze drying. Carbon 39 (2001): 2369 –2386.
- [28] Shaheen, A., Muhtaseb, A., and James, A. Preparation and properties of resorcinol-formaldehyde organics and carbon gels. Advanced Materials 15(2) (2003): 101-114.
- [29] Job, N., Pirard, R., Marien, J., and Pirard, J.P. Porous carbon xerogels with texture tailored by pH control during sol-gel process. Carbon 42 (2004): 619-628.
- [30] Tonanon, N., Siyasukh, A., Tanthapanichakoon, W., Nishihara, H., Mukai, S.R., and Tamon, H. Improvement of mesoporosity of carbon xerogels by ultrasonic irradiation. Carbon 43 (2005): 525–531.
- [31] Siyasukh, A., Maneeprom, P., Larpiattaworn, S., Tonanon, N., Tanthapanichakoon, W., Tamon, H., and Charinpanitkul, T. Preparation of a carbon monolith with hierarchical porous structure by ultrasonic

- irradiation followed by carbonization, physical and chemical activation. Carbon 46 (2008): 1309-1315.
- [32] Lee, W.J., and Lan, W.C. Properties of resorcinol-tannin-formaldehyde copolymer resins prepared from the bark extracts of Taiwan acacia and China fir. Bioresource Technology 97 (2006): 257–264.
- [33] Szczurek, A., Amaral-Labat, G., Fierro, V., Pizzi, A., Mason, E., and Celzard, A. The use of tannin to prepare carbon gels. Part I: Carbon aerogels. Carbon 49 (2011): 2773-2784.
- [34] Szczurek, A., Amaral-Labat, G., Fierro, V., Pizzi, A., and Celzard, A. The use of tannin to prepare carbon gels. Part II: Carbon aerogels. Carbon 49 (2011): 2784-2794.
- [35] Garrote, G., Falque', E., Dominquez, H., and Parajo, J.C. Autohydrolysis of agricultural residues: Study of reaction by product. Bioresource Technology 98 (2007): 1951-1957.
- [36] Wang, Y., and Deng, Y. The kinetics of cellulose dissolution in sodium hydroxide solution at low temperature. Biotechnology and Bioengineering 102 (2009): 1398-1405.
- [37] Yang, H., Yan, R., Chen, H., Lee, D.H., and Zheng, C. Characteristics of hemicelluloses, cellulose and lignin pyrolysis. Fuel 86 (2007): 1781-1788.



## **APPENDIX**

### Properties of carbon monoliths

Table 1: N<sub>2</sub> Adsorption-Desorption Isotherm at 77K of C-RF monolith

| Adsorption |                                             | Desorption |                                             |
|------------|---------------------------------------------|------------|---------------------------------------------|
| $p/p_0$    | $V_a/\text{cm}^3(\text{STP}) \text{g}^{-1}$ | $p/p_0$    | $V_a/\text{cm}^3(\text{STP}) \text{g}^{-1}$ |
| 6.641E-05  | 0.12                                        | 9.661E-01  | 148.70                                      |
| 1.328E-04  | 0.20                                        | 9.384E-01  | 148.59                                      |
| 1.328E-04  | 0.27                                        | 8.811E-01  | 148.29                                      |
| 1.992E-04  | 0.49                                        | 8.346E-01  | 147.98                                      |
| 1.992E-04  | 0.71                                        | 7.836E-01  | 147.64                                      |
| 1.328E-04  | 1.17                                        | 7.341E-01  | 147.29                                      |
| 1.992E-04  | 1.63                                        | 6.843E-01  | 146.91                                      |
| 2.656E-04  | 7.18                                        | 6.343E-01  | 146.51                                      |
| 2.656E-04  | 13.03                                       | 5.847E-01  | 146.09                                      |
| 3.321E-04  | 19.17                                       | 5.351E-01  | 145.63                                      |
| 2.656E-04  | 25.64                                       | 4.853E-01  | 145.14                                      |
| 3.321E-04  | 32.43                                       | 4.354E-01  | 144.64                                      |
| 4.649E-04  | 39.55                                       | 3.862E-01  | 144.08                                      |
| 4.649E-04  | 47.04                                       | 3.368E-01  | 143.44                                      |
| 5.313E-04  | 54.91                                       | 2.878E-01  | 142.69                                      |
| 7.305E-04  | 63.16                                       | 2.700E-01  | 142.19                                      |
| 9.297E-04  | 71.79                                       | 2.424E-01  | 141.66                                      |
| 1.395E-03  | 80.77                                       | 2.185E-01  | 141.13                                      |
| 2.524E-03  | 90.00                                       | 1.937E-01  | 140.55                                      |
| 4.914E-03  | 99.23                                       | 1.693E-01  | 139.89                                      |
| 1.109E-02  | 107.88                                      | 1.451E-01  | 139.15                                      |
| 1.913E-02  | 115.31                                      | 1.211E-01  | 138.28                                      |
| 3.254E-02  | 120.88                                      | 9.775E-02  | 137.21                                      |
| 3.998E-02  | 124.40                                      |            |                                             |
| 4.416E-02  | 126.67                                      |            |                                             |
| 4.748E-02  | 128.14                                      |            |                                             |
| 8.839E-02  | 130.89                                      |            |                                             |
| 1.011E-01  | 132.89                                      |            |                                             |
| 1.448E-01  | 134.91                                      |            |                                             |

| Adsorption |                                              | Desorption |                                              |
|------------|----------------------------------------------|------------|----------------------------------------------|
| $p/p_0$    | $V_a/\text{cm}^3(\text{STP}) \text{ g}^{-1}$ | $p/p_0$    | $V_a/\text{cm}^3(\text{STP}) \text{ g}^{-1}$ |
| 1.509E-01  | 136.10                                       |            |                                              |
| 2.045E-01  | 137.53                                       |            |                                              |
| 2.513E-01  | 138.97                                       |            |                                              |
| 3.115E-01  | 140.31                                       |            |                                              |
| 3.866E-01  | 141.64                                       |            |                                              |
| 4.028E-01  | 142.40                                       |            |                                              |
| 4.669E-01  | 143.14                                       |            |                                              |
| 5.114E-01  | 143.86                                       |            |                                              |
| 5.644E-01  | 144.49                                       |            |                                              |
| 6.137E-01  | 145.09                                       |            |                                              |
| 6.639E-01  | 145.59                                       |            |                                              |
| 7.148E-01  | 146.08                                       |            |                                              |
| 7.644E-01  | 146.58                                       |            |                                              |
| 8.148E-01  | 147.06                                       |            |                                              |
| 8.649E-01  | 147.52                                       |            |                                              |
| 9.150E-01  | 147.96                                       |            |                                              |
| 9.651E-01  | 148.38                                       |            |                                              |
| 9.814E-01  | 148.65                                       |            |                                              |

Table 2: N<sub>2</sub> Adsorption-Desorption Isotherm at 77K of C-L (4:1) monolith

| Adsorption |                                             | Desorption |                                             |
|------------|---------------------------------------------|------------|---------------------------------------------|
| $p/p_0$    | $V_a/\text{cm}^3(\text{STP}) \text{g}^{-1}$ | $p/p_0$    | $V_a/\text{cm}^3(\text{STP}) \text{g}^{-1}$ |
| 4.108E-05  | 0.06                                        | 9.542E-01  | 324.48                                      |
| 4.108E-05  | 0.06                                        | 8.726E-01  | 322.61                                      |
| 8.215E-05  | 0.12                                        | 8.413E-01  | 320.93                                      |
| 1.232E-04  | 8.56                                        | 7.998E-01  | 316.44                                      |
| 2.054E-04  | 17.43                                       | 7.735E-01  | 307.89                                      |
| 2.465E-04  | 26.75                                       | 7.771E-01  | 301.01                                      |
| 3.286E-04  | 36.54                                       | 7.713E-01  | 294.73                                      |
| 4.108E-04  | 46.82                                       | 7.703E-01  | 289.08                                      |
| 6.161E-04  | 57.58                                       | 7.681E-01  | 283.82                                      |
| 1.232E-03  | 68.76                                       | 7.670E-01  | 278.94                                      |
| 2.957E-03  | 80.15                                       | 7.655E-01  | 274.37                                      |
| 8.092E-03  | 91.05                                       | 7.642E-01  | 270.11                                      |
| 2.078E-02  | 100.02                                      | 7.633E-01  | 266.10                                      |
| 3.368E-02  | 106.16                                      | 7.619E-01  | 262.39                                      |
| 4.247E-02  | 109.78                                      | 7.613E-01  | 258.86                                      |
| 7.480E-02  | 115.72                                      | 7.603E-01  | 255.56                                      |
| 1.005E-01  | 119.49                                      | 7.594E-01  | 252.49                                      |
| 1.287E-01  | 122.87                                      | 7.588E-01  | 249.57                                      |
| 1.552E-01  | 125.78                                      | 7.551E-01  | 247.30                                      |
| 1.820E-01  | 128.36                                      | 7.548E-01  | 245.40                                      |
| 2.080E-01  | 130.68                                      | 7.151E-01  | 237.62                                      |
| 2.598E-01  | 134.88                                      | 7.273E-01  | 231.49                                      |
| 2.854E-01  | 136.81                                      | 7.170E-01  | 225.82                                      |
| 3.107E-01  | 138.69                                      | 7.176E-01  | 220.95                                      |
| 3.555E-01  | 141.34                                      | 7.140E-01  | 216.53                                      |
| 4.101E-01  | 144.74                                      | 7.126E-01  | 212.63                                      |
| 5.077E-01  | 151.74                                      | 7.109E-01  | 209.13                                      |
| 5.559E-01  | 155.55                                      | 7.092E-01  | 206.00                                      |
| 6.048E-01  | 159.68                                      | 7.076E-01  | 203.30                                      |
| 6.525E-01  | 164.10                                      | 7.031E-01  | 201.41                                      |
| 6.991E-01  | 169.32                                      | 6.567E-01  | 194.95                                      |
| 7.454E-01  | 175.39                                      | 6.631E-01  | 191.73                                      |
| 7.878E-01  | 182.90                                      | 6.618E-01  | 188.04                                      |
| 7.813E-01  | 187.59                                      | 6.573E-01  | 185.11                                      |
| 7.938E-01  | 190.95                                      | 6.527E-01  | 183.31                                      |

| Adsorption |                                             | Desorption |                                             |
|------------|---------------------------------------------|------------|---------------------------------------------|
| $p/p_0$    | $V_a/\text{cm}^3(\text{STP}) \text{g}^{-1}$ | $p/p_0$    | $V_a/\text{cm}^3(\text{STP}) \text{g}^{-1}$ |
| 7.927E-01  | 193.34                                      | 6.006E-01  | 177.71                                      |
| 7.972E-01  | 195.17                                      | 5.580E-01  | 171.19                                      |
| 8.459E-01  | 201.21                                      | 5.596E-01  | 168.32                                      |
| 8.718E-01  | 217.65                                      | 5.550E-01  | 165.91                                      |
| 8.802E-01  | 223.80                                      | 5.498E-01  | 164.74                                      |
| 8.820E-01  | 228.97                                      | 4.912E-01  | 160.74                                      |
| 8.873E-01  | 237.39                                      | 4.486E-01  | 156.43                                      |
| 8.888E-01  | 240.90                                      | 3.973E-01  | 151.63                                      |
| 8.907E-01  | 244.00                                      | 3.451E-01  | 147.22                                      |
| 8.920E-01  | 246.77                                      | 2.929E-01  | 143.36                                      |
| 8.939E-01  | 251.53                                      | 2.736E-01  | 141.17                                      |
| 9.355E-01  | 260.73                                      | 2.441E-01  | 139.10                                      |
| 9.265E-01  | 266.15                                      | 2.203E-01  | 137.27                                      |
| 9.336E-01  | 271.30                                      | 1.951E-01  | 135.37                                      |
| 9.342E-01  | 275.73                                      | 1.705E-01  | 133.43                                      |
| 9.372E-01  | 283.60                                      | 1.460E-01  | 131.37                                      |
| 9.399E-01  | 290.30                                      | 1.219E-01  | 129.14                                      |
| 9.410E-01  | 293.21                                      | 9.825E-02  | 126.61                                      |
| 9.420E-01  | 295.87                                      |            |                                             |
| 9.425E-01  | 298.35                                      |            |                                             |
| 9.434E-01  | 300.67                                      |            |                                             |
| 9.440E-01  | 302.84                                      |            |                                             |
| 9.448E-01  | 304.81                                      |            |                                             |
| 9.453E-01  | 306.66                                      |            |                                             |
| 9.679E-01  | 311.04                                      |            |                                             |
| 9.630E-01  | 314.13                                      |            |                                             |
| 9.682E-01  | 316.91                                      |            |                                             |
| 9.681E-01  | 319.25                                      |            |                                             |
| 9.710E-01  | 321.19                                      |            |                                             |
| 9.901E-01  | 323.63                                      |            |                                             |

Table 3: N<sub>2</sub> Adsorption-Desorption Isotherm at 77K of C-L (1:1) monolith

| Adsorption |                                             | Desorption |                                             |
|------------|---------------------------------------------|------------|---------------------------------------------|
| $p/p_0$    | $V_a/\text{cm}^3(\text{STP}) \text{g}^{-1}$ | $p/p_0$    | $V_a/\text{cm}^3(\text{STP}) \text{g}^{-1}$ |
| 2.888E-04  | 0.00                                        | 9.700E-01  | 2.26                                        |
| 6.601E-04  | 0.00                                        | 9.450E-01  | 2.11                                        |
| 5.495E-02  | 0.01                                        | 8.960E-01  | 1.87                                        |
| 7.995E-02  | 0.03                                        | 8.460E-01  | 1.65                                        |
| 1.050E-01  | 0.04                                        | 7.958E-01  | 1.44                                        |
| 1.300E-01  | 0.05                                        | 7.459E-01  | 1.25                                        |
| 1.550E-01  | 0.07                                        | 6.958E-01  | 1.07                                        |
| 1.799E-01  | 0.09                                        | 6.457E-01  | 0.90                                        |
| 2.049E-01  | 0.11                                        | 5.957E-01  | 0.76                                        |
| 2.299E-01  | 0.13                                        | 5.456E-01  | 0.63                                        |
| 2.549E-01  | 0.16                                        | 4.955E-01  | 0.50                                        |
| 2.799E-01  | 0.19                                        | 4.455E-01  | 0.40                                        |
| 3.049E-01  | 0.22                                        | 3.954E-01  | 0.30                                        |
| 3.545E-01  | 0.29                                        | 3.453E-01  | 0.22                                        |
| 4.047E-01  | 0.38                                        | 2.952E-01  | 0.15                                        |
| 4.546E-01  | 0.47                                        | 2.701E-01  | 0.12                                        |
| 5.044E-01  | 0.58                                        | 2.450E-01  | 0.09                                        |
| 5.544E-01  | 0.71                                        | 2.200E-01  | 0.07                                        |
| 6.042E-01  | 0.84                                        | 1.950E-01  | 0.05                                        |
| 6.541E-01  | 0.99                                        | 1.700E-01  | 0.04                                        |
| 7.040E-01  | 1.16                                        | 1.450E-01  | 0.03                                        |
| 7.539E-01  | 1.33                                        | 1.200E-01  | 0.02                                        |
| 8.038E-01  | 1.51                                        | 9.497E-02  | 0.01                                        |
| 8.536E-01  | 1.71                                        |            |                                             |
| 9.035E-01  | 1.94                                        |            |                                             |
| 9.533E-01  | 2.18                                        |            |                                             |
| 9.790E-01  | 2.30                                        |            |                                             |
| 9.944E-01  | 2.40                                        |            |                                             |

Table 4: N<sub>2</sub> Adsorption-Desorption Isotherm at 77K of C-H (4:1) monolith

| Adsorption |                                              | Desorption |                                              |
|------------|----------------------------------------------|------------|----------------------------------------------|
| $p/p_0$    | $V_a/\text{cm}^3(\text{STP}) \text{ g}^{-1}$ | $p/p_0$    | $V_a/\text{cm}^3(\text{STP}) \text{ g}^{-1}$ |
| 1.220E-04  | 0.03                                         | 9.697E-01  | 4.28                                         |
| 2.439E-04  | 0.05                                         | 9.452E-01  | 3.94                                         |
| 5.423E-02  | 0.20                                         | 8.960E-01  | 3.54                                         |
| 7.976E-02  | 0.25                                         | 8.455E-01  | 3.25                                         |
| 1.049E-01  | 0.28                                         | 7.950E-01  | 2.99                                         |
| 1.299E-01  | 0.31                                         | 7.453E-01  | 2.76                                         |
| 1.548E-01  | 0.35                                         | 6.950E-01  | 2.57                                         |
| 1.799E-01  | 0.38                                         | 6.449E-01  | 2.39                                         |
| 2.048E-01  | 0.42                                         | 5.951E-01  | 2.24                                         |
| 2.298E-01  | 0.46                                         | 5.451E-01  | 2.11                                         |
| 2.548E-01  | 0.50                                         | 4.950E-01  | 2.02                                         |
| 2.797E-01  | 0.56                                         | 4.450E-01  | 1.93                                         |
| 3.047E-01  | 0.61                                         | 3.950E-01  | 1.85                                         |
| 3.545E-01  | 0.70                                         | 3.449E-01  | 1.79                                         |
| 4.046E-01  | 0.81                                         | 2.949E-01  | 1.75                                         |
| 4.545E-01  | 0.95                                         | 2.699E-01  | 1.75                                         |
| 5.043E-01  | 1.11                                         | 2.449E-01  | 1.75                                         |
| 5.541E-01  | 1.30                                         | 2.199E-01  | 1.76                                         |
| 6.039E-01  | 1.50                                         | 1.948E-01  | 1.77                                         |
| 6.540E-01  | 1.74                                         | 1.699E-01  | 1.78                                         |
| 7.038E-01  | 2.00                                         | 1.449E-01  | 1.80                                         |
| 7.536E-01  | 2.28                                         | 1.199E-01  | 1.82                                         |
| 8.034E-01  | 2.59                                         | 9.493E-02  | 1.84                                         |
| 8.532E-01  | 2.93                                         |            |                                              |
| 9.029E-01  | 3.32                                         |            |                                              |
| 9.524E-01  | 3.79                                         |            |                                              |
| 9.779E-01  | 4.17                                         |            |                                              |
| 9.930E-01  | 4.50                                         |            |                                              |

Table 5: N<sub>2</sub> Adsorption-Desorption Isotherm at 77K of C-H (1:1) monolith

| Adsorption |                                             | Desorption |                                             |
|------------|---------------------------------------------|------------|---------------------------------------------|
| $p/p_0$    | $V_a/\text{cm}^3(\text{STP}) \text{g}^{-1}$ | $p/p_0$    | $V_a/\text{cm}^3(\text{STP}) \text{g}^{-1}$ |
| 8.102E-05  | 0.01                                        | 9.709E-01  | 3.90                                        |
| 5.068E-02  | 0.40                                        | 9.477E-01  | 3.42                                        |
| 7.948E-02  | 0.46                                        | 8.980E-01  | 2.89                                        |
| 1.048E-01  | 0.49                                        | 8.454E-01  | 2.51                                        |
| 1.298E-01  | 0.51                                        | 7.951E-01  | 2.21                                        |
| 1.548E-01  | 0.55                                        | 7.460E-01  | 1.98                                        |
| 1.799E-01  | 0.57                                        | 6.951E-01  | 1.77                                        |
| 2.049E-01  | 0.59                                        | 6.457E-01  | 1.59                                        |
| 2.299E-01  | 0.62                                        | 5.952E-01  | 1.42                                        |
| 2.548E-01  | 0.65                                        | 5.456E-01  | 1.27                                        |
| 2.798E-01  | 0.68                                        | 4.951E-01  | 1.14                                        |
| 3.048E-01  | 0.71                                        | 4.453E-01  | 1.01                                        |
| 3.544E-01  | 0.78                                        | 3.952E-01  | 0.91                                        |
| 4.045E-01  | 0.87                                        | 3.451E-01  | 0.82                                        |
| 4.544E-01  | 0.98                                        | 2.951E-01  | 0.74                                        |
| 5.042E-01  | 1.08                                        | 2.700E-01  | 0.71                                        |
| 5.541E-01  | 1.21                                        | 2.450E-01  | 0.68                                        |
| 6.040E-01  | 1.35                                        | 2.200E-01  | 0.65                                        |
| 6.536E-01  | 1.51                                        | 1.950E-01  | 0.63                                        |
| 7.038E-01  | 1.70                                        | 1.700E-01  | 0.60                                        |
| 7.531E-01  | 1.92                                        | 1.451E-01  | 0.57                                        |
| 8.035E-01  | 2.16                                        | 1.201E-01  | 0.55                                        |
| 8.526E-01  | 2.42                                        | 9.508E-02  | 0.52                                        |
| 9.027E-01  | 2.76                                        |            |                                             |
| 9.508E-01  | 3.24                                        |            |                                             |
| 9.768E-01  | 3.69                                        |            |                                             |
| 9.916E-01  | 4.14                                        |            |                                             |



Table 6: N<sub>2</sub> Adsorption-Desorption Isotherm at 77K of C-LCM (4:1) monolith

| Adsorption |                                             | Desorption |                                             |
|------------|---------------------------------------------|------------|---------------------------------------------|
| $p/p_0$    | $V_a/\text{cm}^3(\text{STP}) \text{g}^{-1}$ | $p/p_0$    | $V_a/\text{cm}^3(\text{STP}) \text{g}^{-1}$ |
| 5.472E-19  | 0.03                                        | 9.706E-01  | 4.98                                        |
| 5.472E-19  | 0.06                                        | 9.469E-01  | 4.60                                        |
| 8.249E-05  | 0.08                                        | 8.978E-01  | 4.10                                        |
| 8.249E-05  | 0.12                                        | 8.456E-01  | 3.71                                        |
| 8.249E-05  | 0.15                                        | 7.963E-01  | 3.42                                        |
| 2.887E-04  | 0.20                                        | 7.454E-01  | 3.18                                        |
| 1.320E-03  | 0.31                                        | 6.957E-01  | 2.98                                        |
| 5.292E-02  | 0.59                                        | 6.455E-01  | 2.81                                        |
| 7.940E-02  | 0.70                                        | 5.954E-01  | 2.66                                        |
| 1.047E-01  | 0.76                                        | 5.454E-01  | 2.54                                        |
| 1.548E-01  | 0.86                                        | 4.950E-01  | 2.42                                        |
| 1.799E-01  | 0.90                                        | 4.451E-01  | 2.29                                        |
| 2.049E-01  | 0.96                                        | 3.948E-01  | 2.21                                        |
| 2.549E-01  | 1.06                                        | 3.447E-01  | 2.14                                        |
| 2.799E-01  | 1.12                                        | 2.947E-01  | 2.09                                        |
| 3.049E-01  | 1.17                                        | 2.698E-01  | 2.06                                        |
| 3.547E-01  | 1.26                                        | 2.447E-01  | 2.05                                        |
| 4.050E-01  | 1.38                                        | 2.198E-01  | 2.03                                        |
| 4.549E-01  | 1.50                                        | 1.947E-01  | 2.02                                        |
| 5.048E-01  | 1.64                                        | 1.698E-01  | 2.01                                        |
| 5.546E-01  | 1.80                                        | 1.447E-01  | 2.00                                        |
| 6.045E-01  | 1.98                                        | 1.198E-01  | 1.99                                        |
| 6.543E-01  | 2.19                                        | 9.478E-02  | 1.97                                        |
| 7.041E-01  | 2.40                                        |            |                                             |
| 7.540E-01  | 2.66                                        |            |                                             |
| 8.038E-01  | 2.94                                        |            |                                             |
| 8.531E-01  | 3.27                                        |            |                                             |
| 9.032E-01  | 3.69                                        |            |                                             |
| 9.515E-01  | 4.22                                        |            |                                             |
| 9.772E-01  | 4.71                                        |            |                                             |

Table 7: N<sub>2</sub> Adsorption-Desorption Isotherm at 77K of C-LCM (1:1) monolith

| Adsorption |                                             | Desorption |                                             |
|------------|---------------------------------------------|------------|---------------------------------------------|
| $p/p_0$    | $V_a/\text{cm}^3(\text{STP}) \text{g}^{-1}$ | $p/p_0$    | $V_a/\text{cm}^3(\text{STP}) \text{g}^{-1}$ |
| 8.216E-19  | 0.04                                        | 9.594E-01  | 139.20                                      |
| 8.216E-19  | 0.07                                        | 9.438E-01  | 138.52                                      |
| 4.070E-05  | 0.11                                        | 8.836E-01  | 136.78                                      |
| 4.070E-05  | 0.16                                        | 8.389E-01  | 135.06                                      |
| 4.070E-05  | 0.23                                        | 7.834E-01  | 133.67                                      |
| 8.216E-19  | 0.45                                        | 7.342E-01  | 132.58                                      |
| 4.070E-05  | 0.68                                        | 6.828E-01  | 131.66                                      |
| 8.140E-05  | 8.38                                        | 6.330E-01  | 130.83                                      |
| 1.628E-04  | 16.46                                       | 5.825E-01  | 130.05                                      |
| 2.442E-04  | 24.94                                       | 5.324E-01  | 129.32                                      |
| 4.477E-04  | 33.82                                       | 4.830E-01  | 128.55                                      |
| 8.547E-04  | 43.03                                       | 4.403E-01  | 126.84                                      |
| 2.117E-03  | 52.42                                       | 3.872E-01  | 124.98                                      |
| 4.681E-03  | 61.64                                       | 3.352E-01  | 123.61                                      |
| 9.606E-03  | 70.17                                       | 2.848E-01  | 122.45                                      |
| 1.791E-02  | 77.51                                       | 2.698E-01  | 121.75                                      |
| 2.837E-02  | 83.19                                       | 2.393E-01  | 121.08                                      |
| 3.647E-02  | 87.36                                       | 2.169E-01  | 120.46                                      |
| 3.924E-02  | 90.62                                       | 1.908E-01  | 119.81                                      |
| 4.209E-02  | 93.29                                       | 1.668E-01  | 119.10                                      |
| 4.400E-02  | 95.48                                       | 1.418E-01  | 118.33                                      |
| 4.587E-02  | 97.26                                       | 1.177E-01  | 117.44                                      |
| 7.921E-02  | 100.20                                      | 9.349E-02  | 116.40                                      |
| 9.915E-02  | 103.16                                      |            |                                             |
| 1.308E-01  | 105.94                                      |            |                                             |
| 1.544E-01  | 108.30                                      |            |                                             |
| 1.835E-01  | 110.39                                      |            |                                             |
| 2.080E-01  | 112.15                                      |            |                                             |
| 2.359E-01  | 113.70                                      |            |                                             |
| 2.600E-01  | 115.06                                      |            |                                             |
| 2.878E-01  | 116.28                                      |            |                                             |
| 3.115E-01  | 117.34                                      |            |                                             |
| 3.606E-01  | 118.51                                      |            |                                             |
| 4.162E-01  | 119.84                                      |            |                                             |
| 4.639E-01  | 121.07                                      |            |                                             |

| Adsorption |                                              | Desorption |                                              |
|------------|----------------------------------------------|------------|----------------------------------------------|
| $p/p_0$    | $V_a/\text{cm}^3(\text{STP}) \text{ g}^{-1}$ | $p/p_0$    | $V_a/\text{cm}^3(\text{STP}) \text{ g}^{-1}$ |
| 5.158E-01  | 122.21                                       |            |                                              |
| 5.651E-01  | 123.31                                       |            |                                              |
| 6.156E-01  | 124.38                                       |            |                                              |
| 6.658E-01  | 125.38                                       |            |                                              |
| 7.146E-01  | 126.53                                       |            |                                              |
| 7.647E-01  | 127.76                                       |            |                                              |
| 8.135E-01  | 129.13                                       |            |                                              |
| 8.627E-01  | 130.69                                       |            |                                              |
| 9.113E-01  | 132.49                                       |            |                                              |
| 9.583E-01  | 134.77                                       |            |                                              |
| 9.730E-01  | 136.87                                       |            |                                              |
| 9.886E-01  | 138.89                                       |            |                                              |

Table 8: N<sub>2</sub> Adsorption-Desorption Isotherm at 77K of C-LH (4:1) monolith

| Adsorption |                                             | Desorption |                                             |
|------------|---------------------------------------------|------------|---------------------------------------------|
| $p/p_0$    | $V_a/\text{cm}^3(\text{STP}) \text{g}^{-1}$ | $p/p_0$    | $V_a/\text{cm}^3(\text{STP}) \text{g}^{-1}$ |
| 8.239E-05  | 0.02                                        | 9.689E-01  | 12.78                                       |
| 8.239E-05  | 0.06                                        | 9.502E-01  | 11.84                                       |
| 4.120E-05  | 0.10                                        | 9.046E-01  | 10.21                                       |
| 8.239E-05  | 0.13                                        | 8.493E-01  | 8.64                                        |
| 8.239E-05  | 0.17                                        | 7.992E-01  | 7.75                                        |
| 8.239E-05  | 0.23                                        | 7.461E-01  | 7.20                                        |
| 2.060E-04  | 0.43                                        | 6.952E-01  | 6.82                                        |
| 4.943E-04  | 0.64                                        | 6.449E-01  | 6.52                                        |
| 1.936E-03  | 0.90                                        | 5.945E-01  | 6.27                                        |
| 5.104E-02  | 1.55                                        | 5.443E-01  | 6.07                                        |
| 7.827E-02  | 1.85                                        | 4.941E-01  | 5.90                                        |
| 1.040E-01  | 2.06                                        | 4.441E-01  | 5.74                                        |
| 1.292E-01  | 2.24                                        | 3.939E-01  | 5.62                                        |
| 1.544E-01  | 2.39                                        | 3.439E-01  | 5.51                                        |
| 1.795E-01  | 2.54                                        | 2.938E-01  | 5.43                                        |
| 2.046E-01  | 2.68                                        | 2.694E-01  | 5.39                                        |
| 2.547E-01  | 2.98                                        | 2.444E-01  | 5.36                                        |
| 2.797E-01  | 3.14                                        | 2.193E-01  | 5.34                                        |
| 3.048E-01  | 3.27                                        | 1.943E-01  | 5.32                                        |
| 3.544E-01  | 3.47                                        | 1.694E-01  | 5.30                                        |
| 4.553E-01  | 3.94                                        | 1.443E-01  | 5.28                                        |
| 5.051E-01  | 4.22                                        | 1.194E-01  | 5.25                                        |
| 5.550E-01  | 4.52                                        | 9.446E-02  | 5.22                                        |
| 6.048E-01  | 4.85                                        |            |                                             |
| 6.546E-01  | 5.22                                        |            |                                             |
| 7.539E-01  | 6.12                                        |            |                                             |
| 8.033E-01  | 6.69                                        |            |                                             |
| 8.524E-01  | 7.40                                        |            |                                             |
| 9.007E-01  | 8.35                                        |            |                                             |
| 9.486E-01  | 9.77                                        |            |                                             |
| 9.712E-01  | 11.21                                       |            |                                             |
| 9.888E-01  | 12.71                                       |            |                                             |

Table 9: N<sub>2</sub> Adsorption-Desorption Isotherm at 77K of C-LH (1:1) monolith

| Adsorption |                                              | Desorption |                                              |
|------------|----------------------------------------------|------------|----------------------------------------------|
| $p/p_0$    | $V_a/\text{cm}^3(\text{STP}) \text{ g}^{-1}$ | $p/p_0$    | $V_a/\text{cm}^3(\text{STP}) \text{ g}^{-1}$ |
| 4.058E-05  | 1.59                                         | 9.664E-01  | 217.82                                       |
| 4.058E-05  | 2.28                                         | 9.482E-01  | 216.06                                       |
| 8.115E-05  | 9.22                                         | 9.096E-01  | 210.55                                       |
| 1.217E-04  | 16.52                                        | 9.117E-01  | 207.75                                       |
| 2.840E-04  | 24.17                                        | 9.118E-01  | 204.71                                       |
| 4.058E-04  | 32.20                                        | 9.080E-01  | 202.10                                       |
| 6.898E-04  | 40.60                                        | 9.031E-01  | 200.43                                       |
| 1.704E-03  | 49.26                                        | 8.579E-01  | 194.75                                       |
| 4.626E-03  | 57.88                                        | 8.621E-01  | 192.06                                       |
| 1.087E-02  | 65.89                                        | 8.639E-01  | 188.73                                       |
| 2.264E-02  | 72.39                                        | 8.589E-01  | 185.87                                       |
| 3.327E-02  | 77.00                                        | 8.582E-01  | 183.48                                       |
| 3.981E-02  | 80.12                                        | 8.515E-01  | 181.98                                       |
| 4.451E-02  | 82.21                                        | 8.032E-01  | 176.97                                       |
| 4.707E-02  | 83.63                                        | 7.623E-01  | 170.73                                       |
| 7.551E-02  | 86.56                                        | 7.703E-01  | 166.63                                       |
| 9.970E-02  | 89.44                                        | 7.576E-01  | 163.46                                       |
| 1.279E-01  | 92.15                                        | 7.534E-01  | 161.83                                       |
| 1.539E-01  | 94.56                                        | 6.986E-01  | 157.21                                       |
| 1.811E-01  | 96.74                                        | 6.557E-01  | 152.11                                       |
| 2.064E-01  | 98.75                                        | 6.579E-01  | 150.13                                       |
| 2.323E-01  | 100.72                                       | 6.533E-01  | 148.52                                       |
| 2.583E-01  | 102.59                                       | 5.941E-01  | 144.45                                       |
| 2.839E-01  | 104.38                                       | 5.500E-01  | 140.37                                       |
| 3.100E-01  | 106.07                                       | 4.954E-01  | 136.38                                       |
| 3.556E-01  | 108.27                                       | 4.487E-01  | 132.41                                       |
| 4.117E-01  | 110.99                                       | 4.015E-01  | 127.90                                       |
| 4.578E-01  | 113.68                                       | 3.488E-01  | 123.44                                       |
| 5.095E-01  | 116.47                                       | 2.945E-01  | 119.69                                       |
| 5.571E-01  | 119.40                                       | 2.757E-01  | 117.49                                       |
| 6.065E-01  | 122.58                                       | 2.435E-01  | 115.68                                       |
| 6.543E-01  | 126.08                                       | 2.198E-01  | 114.29                                       |
| 7.019E-01  | 130.00                                       | 1.936E-01  | 112.92                                       |
| 7.485E-01  | 134.50                                       | 1.693E-01  | 111.57                                       |
| 7.943E-01  | 139.76                                       | 1.443E-01  | 110.18                                       |

| Adsorption |                                              | Desorption |                                              |
|------------|----------------------------------------------|------------|----------------------------------------------|
| $p/p_0$    | $V_a/\text{cm}^3(\text{STP}) \text{ g}^{-1}$ | $p/p_0$    | $V_a/\text{cm}^3(\text{STP}) \text{ g}^{-1}$ |
| 7.836E-01  | 142.74                                       | 1.201E-01  | 108.69                                       |
| 7.972E-01  | 144.90                                       | 9.633E-02  | 106.98                                       |
| 8.488E-01  | 149.65                                       |            |                                              |
| 8.850E-01  | 155.93                                       |            |                                              |
| 8.808E-01  | 159.94                                       |            |                                              |
| 8.875E-01  | 163.43                                       |            |                                              |
| 8.903E-01  | 166.10                                       |            |                                              |
| 8.923E-01  | 168.30                                       |            |                                              |
| 8.947E-01  | 169.91                                       |            |                                              |
| 8.946E-01  | 171.51                                       |            |                                              |
| 8.985E-01  | 172.62                                       |            |                                              |
| 9.414E-01  | 178.07                                       |            |                                              |
| 9.290E-01  | 181.81                                       |            |                                              |
| 9.397E-01  | 185.17                                       |            |                                              |
| 9.378E-01  | 187.94                                       |            |                                              |
| 9.412E-01  | 190.44                                       |            |                                              |
| 9.419E-01  | 192.60                                       |            |                                              |
| 9.436E-01  | 194.49                                       |            |                                              |
| 9.441E-01  | 196.20                                       |            |                                              |
| 9.651E-01  | 201.72                                       |            |                                              |
| 9.604E-01  | 204.77                                       |            |                                              |
| 9.647E-01  | 207.61                                       |            |                                              |
| 9.674E-01  | 209.80                                       |            |                                              |
| 9.687E-01  | 211.63                                       |            |                                              |
| 9.692E-01  | 213.31                                       |            |                                              |
| 9.703E-01  | 214.81                                       |            |                                              |
| 9.803E-01  | 217.96                                       |            |                                              |

## **BIOGRAPHY**

Mr. Rittikrai Nammoonsin was born on August, 1986 in Khon Kaen, Thailand. He graduated with the Bachelor Degree of Science in Chemical Engineering from Department of Chemical Technology, Faculty of Science, Chulalongkorn University in 2008 and furthered his Master's Degree of Engineering in Chemical Engineering Program, Department of Chemical Engineering, Faculty of Engineering, Chulalongkorn University.

During postgraduate studies, his work has been presented in the national level. The presentation was at 1<sup>st</sup> Polymer Conference of Thailand on the topic of "A simple method of lignocellulosic residues dissolution and regeneration" at Chulabhorn Research Institute, Bangkok, Thailand on 7-8 October, 2010.